Delft University of Technology
Faculty of Applied Sciences
Department of Radiation Radionuclides & Reactors
Physics of Nuclear Reactors

Experimental and computational determination of Alpha modes of the Delphi subcritical assembly

Carine Dokter

Supervisors:
dr. ir. Danny Lathouwers
dr. ir. Jan Leen Kloosterman

Delft, June 2012

Abstract

Title: Experimental and computational determination of Alpha modes of the Delphi subcritical assembly

Author: Carine Dokter, Delft University of Technology, Faculty of Applied Sciences, Department of Radiation Radionuclides & Reactors, Group Physics of Nuclear Reactors

The Reactor Institute Delft (RID) owns a subcritical reactor, called Delphi, that is built for training and research purposes. A subcritical reactor is a nuclear fission reactor that is unable to sustain a fission chain reaction since more neutrons are lost, due to absorption and leakage, than produced. A subcritical reactor needs an external neutron source to maintain a steady state fission chain reaction. For safety reasons, a method for reactivity monitoring is required.

The reactivity can be determined by the rate at which the associated flux shape will decay in absence of a source. This time decay constant is called alpha and belongs to the alpha mode. The aim of this research was to determine alpha computationally and by measurements and to give a global comparison of the results.

First the neutrons diffusion equation is rewritten as an eigenvalue problem, and numerically solved by DALTON, a code to solve 3D multi-group diffusion equations on structured grids. To solve the eigenvalue problem, an accurate description of Delphi geometry was required.

After that alpha is measured with the Feynman-α technique, a statistical method to extract alpha from the variance-to-mean ratio of detected neutrons, as function from time intervals. Prior to the measurements an additional study is done to determine the most favourable detector position.

The measurement results and the computational results does not contradict each other. However, to guarantee the accuracy of the measurements and the calculations further research is required.

Table of contents

1. Introduction 4
1.1 General introduction 4
1.2 Delphi subcritical assembly 5
1.3 The objective and structure of this thesis 5
2. Theory of subcritical reactors 6
2.1 Reactivity and alpha modes 6
2.2 Alpha eigenvalue problem 7
2.3 Noise Measurements 9
2.3.1 Rossi Alpha 9
2.3.2 Feynman Alpha 10
2.4 Delphi subcritical assembly. 11
3. Alpha mode calculations 13
3.1 Determining alpha 13
3.2 Basic principles of DALTON 13
3.3 Cross sections generation 13
3.4 The grid used for the DALTON calculations 15
4. Mode measurements 18
4.1 Instrumentation 18
4.2 Detector positions 19
4.3 Dead time correction and error 27
5. Results 29
5.1 Computational results 29
5.2 Results of noise measurements 32
5.3 Comparing measurement and computational results 36
6. Conclusions and Recommendations 38
6.1 Conclusions 38
6.2 Recommendations 39
Appendix 1. External Source ^{252}Cf 40
Appendix 2. Determining energy groups 41
Appendix 3. SCALE input 43
Appendix 4. Matlab script for detector positioning 44
Bibliography ..... **Fout! Bladwijzer niet gedefinieerd.**

1. Introduction

1.1 General introduction

A subcritical reactor is a nuclear fission reactor that does not achieve criticality. The reactor is unable to sustain a fission chain reaction since more neutrons are lost, due to absorption and leakage, than produced. A subcritical reactor needs an external neutron source to maintain a steady state fission chain reaction. The neutron source can be provided by a radioactive isotope which emits neutrons during decay. Another example of a neutron source is an accelerator that produces neutrons by spallation. An accelerator driven system (ADS) is a coupled accelerator to a nuclear reactor. The fast neutrons produced by spallation (1-20MeV) have enough energy to reduce the lifetime of actinide waste, since the probability for high-energy neutrons of causing a fission reaction with actinides is bigger than causing a capture reaction. By fission the actinides transform into radionuclides that, in a majority of cases, are short-lived, or even stable. The nuclei yielded by fission undergo on average four decays, with a half-life not longer than a few years before they reach a stable form. Through capture, the same heavy nuclei transform into other radionuclides, often long-lived. Because of the possibility of transmuting nuclear waste, there is much research on accelerator driven systems. With a sub-critical reactor, the reaction will extinguish unless there are continuously added neutrons from an external source. This can be seen as an advantage in case of emergency.

The difficulty lies in that the subcriticality must be guaranteed. To this end, the reactivity has to be determined in order to exclude that a critical or supercritical configuration occurs. Unfortunately, this does not happen in the same way as in a critical reactor, since the shape of the neutron flux in a subcritical reactor is different from a conventional reactor due to its external source.

The criticality of the system can be measured by the rate at which the associated flux-shape will decay in the absence of a source. This time decay constant is called alpha and belongs to the alpha mode. The time decay constant of a subcritical reactor can be analyzed numerically by solving the time-dependent neutron transport equation directly. This is an expensive method, from a computational point of view. High-dimensional partial differential equation must be solved to describe the time-dependent neutron flux. Another, less expensive method to determine the alpha modes, is to rewrite the neutrons diffusion equation as an eigenvalue problem. This eigenvalue problem can be solved numerically with DALTON, a code that is able to solve the 3D multi-group diffusion equations on structured grids.

Another method for determining alpha, is by measurements. There are several neutron counting techniques in nuclear reactor systems that are sufficient to provide alpha. To measure a useful signal it is important that the neutrons measured originate from the same chain reaction. Therefore, a condition for these measurements is that the power level of the reactor approaches zero.

The purpose of this research is to determine the alpha mode of a subcritical reactor both computationally and by measurements. Due to the above requirement that a zero power reactor is necessary to provide usable measurement results, it is not possible to do the measurements at a power ADS. Therefore, the measurements and calculations are performed with the research reactor Delphi.

1.2 Delphi subcritical assembly

The Reactor Institute Delft (RID) owns a subcritical reactor, called Delphi. It is located in the reactor hall next to the 2MW research reactor. This subcritical reactor Delphi was built for training and research purposes. This subcritical reactor satisfies the requirement for several neutron counting techniques for random noise calculations, since Delphi is a zero power reactor.

The external source is provided by the isotope californium-252. Delphi consists of two vessels one upon the other. The lower vessel is made of stainless steel and is filled with water. The upper acrylic air-filled vessel is used to store 168 fuel pins that can be lowered one after the other. Below the steel vessel, a shielding box is positioned containing the ^{252}Cf-neutron source that can pneumatically be inserted to its experimental position.

1.3 The objective and structure of this thesis

This research was performed as part of the Master Science Education and Communication at the faculty of applied sciences, in the group Physics of Nuclear Reactors at Delft University of Technology. The main objective of this project is to determine the alpha modes of the subcritical reactor Delphi by measurements and calculations and provide a global comparison between the measurement results and the calculated results, provided by DALTON. An additional study is done to determine the most suitable position of the detectors for measuring alpha.

This thesis starts with a theoretical explanation of what the alpha modes are, followed by a mathematical derivation of alpha and the theoretical section on the measurement methods. After that the preparations to calculate alpha with DALTON are discussed. With the results of DALTON, the flux shape is constructed. This data is used to determine the optimal position to place the detectors. After that measurements have been taken. The raw data is processed to extract alpha.

In chapter five the results of the measurements and calculations are presented, discussed and compared. The report closes with conclusions and recommendations for further research.

2. Theory of subcritical reactors

For efficient transmutation of plutonium and for radio-toxicity reductions of minor actinides, fast neutron systems should be used. Given the probability for fast neutrons (1-20MeV) of causing a fission reaction with actinides is bigger than causing a capture reaction. By fission the actinides transform into radionuclides that are short-lived or even stable. In a capture reaction the same heavy nuclei transform into other radionuclides, often long-lived. However, fast reactors suffer from strict safety parameters when loaded with large fractions of plutonium and minor actinides, in particular ^{241}Am. [1] Therefore subcritical reactors might be used. The margin to criticality must be chosen large enough, because criticality must be avoided under all circumstances. Therefore, monitoring of the subcriticality is essential for maintaining safe operation. In this chapter it is explained how the subcriticality can be determined by measurement techniques and by computational means. Therefore the reactivity and the time decay constants will be mathematically derived. After that, techniques to measure this time decay constant will be introduced. Finally a detailed description of Delphi will follow, as an accurate description of Delphi is needed to calculate and measure the reactivity in Delphi.

2.1 Reactivity and alpha modes

One of the most important tasks of a nuclear reactor physicist is to determine the criticality of a nuclear reactor. This is mostly done by determining the multiplication factor, the ratio of rate of neutron production in a nuclear reactor, to the rate of neutron loss in the reactor. By determining the multiplication factor, k_{eff}, the reactivity of the system can be determined.

The reactivity ρ is given by

$$\rho = \frac{k_{eff} - 1}{k_{eff}} \tag{2.1}$$

When ρ>0, the reactor is supercritical, when ρ<0, the reactor is subcritical and when ρ=0 the reactor is critical. In a subcritical reactor it is not possible to determine k_{eff} directly. Therefore it is necessary to use another equation to derive the reactivity expressed by other variables. The point kinetic equations [2] reads

$$\frac{\partial n(t)}{\partial t} = \frac{\rho(t) - \beta}{\Lambda} n(t) + \sum_{i=1}^{6} \lambda_i c_i(t) \tag{2.2}$$

where $n(t)$ is the number of neutrons at time t, β is the total fraction of fission neutrons which are delayed, λ_i c_i is the number of precursors decaying by emitting a delayed neutron per second, and Λ represents the mean neutron generation time.

Assuming that the delayed neutrons can be neglected, the original equation reads as

$$\frac{\partial n(t)}{\partial t} = \alpha n(t) \tag{2.3}$$

with general solution

$$n(t) = c_1 e^{\alpha t} \tag{2.4}$$

where α is the rate of change of the neutron count in the core. This type of differential equation describes exponential growth or exponential decay, depending on the sign of the constant. If α is positive, then the core is supercritical and the rate of neutron production will grow exponentially until some other effect stops the growth. If is negative, then the core is subcritical and the number of free neutrons in the core will shrink exponentially until it reaches zero. If α is exactly zero, then the reactor is critical and its output does not vary in time.

From (2.2) it is clear that

$$\alpha = \frac{\rho(t) - \beta}{\Lambda} \tag{2.5}$$

So, by determining alpha, the reactivity can be determined.

2.2 Alpha eigenvalue problem

To determine the multiplication factor, the number of free neutrons and their behaviour have to be determined. This is achieved by describing the motion of neutrons in the reactor and their interactions with the present materials. The rate of change of number of neutrons in a volume can be calculated by describing the neutron losses and gain in a volume.

The neutron losses are caused by leakage, absorption and scattering. The neutron gain is caused by any neutron sources (external sources and fission) and inscattering. With these terms, a balance equation can be derived, with the rate of change of number of neutrons in a volume at one side, and the gained neutrons and the neutron losses on the other side. [2]

$$\begin{aligned}\left[\int_V \frac{\partial n}{\partial t} dr\right] dE d\hat{\Omega} = &\left[\int_V s(\mathbf{r}, E, \hat{\Omega}, t) dr\right] dE d\hat{\Omega} \ ① \\ &+ \left[\int_V dr \int_{4\pi} d\hat{\Omega}' \int_0^\infty dE' \nu' \Sigma_s(E' \to E, \Omega' \to \Omega) n(\mathbf{r}, E', \hat{\Omega}', t)\right] dE d\hat{\Omega} \ ② \\ &- \left[\int_V dr \nu \hat{\Omega} \cdot \nabla n(\mathbf{r}, E, \hat{\Omega}, t)\right] dE d\hat{\Omega} \ ③ \\ &- \left[\int_V \nu \Sigma_t(\mathbf{r}, E) n(\mathbf{r}, E, \hat{\Omega}, t) d^3 r\right] dE d\hat{\Omega} \ ④\end{aligned} \tag{2.6}$$

Where n represents the density of neutrons, s any neutron sources, Σ_s the macroscopic scattering cross section, ν the average number of neutrons released per fission, Σ_t the macroscopic total cross section.

In this equation ① is the source term, ② is the gain due to scattering into *dE* about *E*, ③ is the leakage into and from the volume V, and ④ is the loss due to collisions.

The distribution of neutrons in a reactor obeys the neutron transport equation, which can be classified as a linear Boltzmann equation. By rewriting the balance equation in terms of a volume integral using Gauss's theorem, and vanish the integral for any *V*, the integrand has to be zero, the neutron transport equation is found.

$$\frac{\partial n}{\partial t} + v\hat{\Omega}\cdot\nabla n + v\Sigma_t n(\mathbf{r},E,\hat{\Omega},t) = \int_{4\pi} d\hat{\Omega}' \int_0^\infty dE'\, v'\Sigma_s(E'\to E,\hat{\Omega}'\to\hat{\Omega}) n(\mathbf{r},E',\hat{\Omega}',t) + s(\mathbf{r},E,\hat{\Omega},t) \tag{2.7}$$

This equation is linear because the neutrons do not have interactions with each other, but only with the material. Because this is an equation with seven degrees of freedom it is very hard to solve. In order to simplify this equation, three approximations have been made. The first is to assume that the angular flux is only weakly dependent on angle, therefore a diffusion approximation is valid, and the equation is integrated over all angles, so the angular dependency vanishes. Then Fick's law is applied, it implies that a spatial variation in the neutron density will give rise to a current of neutrons flowing from regions of high to a low density. The third approximation has to do with the neutron energy. This energy varies from 10 MeV down to less than 0.01 eV. Rather than to treat the neutron energy variable *E* as a continuous variable, the simplified equation discretizes the neutron energies into energy groups. In this project the so called multi group diffusion equation is used. The aim of this project was to provide a global comparison between the measurement results and the calculated results. For that purpose diffusion theory is accurate enough. The multi group diffusion equation is represented by [2]

$$\frac{1}{v_g}\frac{\partial \phi_g}{\partial t} - \nabla\cdot D_g\nabla\phi + \Sigma_{tg}\phi_g(\mathbf{r},t) = \sum_{g'=1}^{G}\Sigma_{sg'g}\phi_{g'} + \chi_g\sum_{g'=1}^{G}\nu_{g'}\Sigma_{fg'}\phi_{g'} + S_g \tag{2.8}$$
$$g = 1,2,.....G$$

Where Φ represents the angular integrated flux, *D* the neutron diffusion coefficient, v_g the neutron speed of group *g*, Σ_t the macroscopic total cross section, Σ_s the scattering cross section, Σ_f the fission cross section, $\chi(E)$ the fission spectrum, *v* the average number of neutrons released per fission and S_g the externals source.

This equation can be written in operator form as

$$\frac{1}{v_g}\frac{\partial \phi_g}{\partial t} = [\mathbf{F}-\mathbf{L}]\phi_g + S_g \tag{2.9}$$

Where the operator **F** describes the fission process and the operator **L** contains the effects of neutron leakage, neutron collisions and the contribution of neutrons scattered into the relevant energy group. Only prompt neutrons are taken into account.

Several eigenvalue problems can be defined from the diffusion equation. The time-eigenvalue gives the rate at which the associated flux-shape, the eigenvector, will decay in the absence of a source. Time eigenvalues can be defined by assuming exponential time behavior of the neutron flux and substituting in the diffusion equation.

$$\Phi(\vec{r},E,t)=\Phi(\vec{r},E)e^{\alpha t} \tag{2.10}$$

By substituting this equation in the multi group diffusion equation the alpha eigenvalue problem is achieved

$$\frac{\alpha}{v}\Phi=[\mathbf{F}-\mathbf{L}]\Phi \tag{2.11}$$

The eigenfunctions following from this problem are the alpha modes.

The general solution to the mathematical description of the neutron flux is a summation over the product of the alpha modes, exponential functions and expansion coefficients.

$$\Phi(\vec{r},E,t)=\sum_{n}A_n e^{\alpha_n t}\Phi_n \tag{2.12}$$

The fundamental mode is the mode associated with the (in magnitude) smallest eigenvalue and this pair describes the flux shape at which the flux will decay or increase (asymptotically) as well as the rate at which the decay or increase proceeds [3].

2.3 Noise Measurements

In a typical subcritical reactor, an artificial neutron source supplies the neutrons necessary to initiate the chain reaction. Each disintegration is an event that is independent of the preceding or following disintegration. Hence the neutrons produced by the reactions with the neutrons from the external source are generated randomly. [4]. The random neutrons may start a fission chain that is not random. Since neutrons gained at a fission event again can lead to a new fission. Depending on the materials in the reactor (coolant, moderator or fuel) this chain is long or short. Ultimately the chain must die out if the reactor is not supercritical. When the reactor is highly subcritical, the neutron chains are quite short and the fluctuations are relatively small. As the reactor approaches criticality, the chains increase in average length. By measuring the neutrons and the time between two detected neutrons, information about the fission chain is gained and therefore information about the reactivity of a reactor. But a distinction has to be made between random neutrons released by the external source and neutrons from a fission chain. This is done by several neutron counting techniques.

2.3.1 Rossi Alpha

Due to fission chain reactions, detected neutrons may be correlated to each other in space and time. It might happen that two neutrons, detected by the same detector, originate from the same fission chain. In this case it is likely that these detections are close in time [1]. The principle of the Rossi-

alpha technique is based on the probability of having one fission event followed by two neutron detections within Δ at $t = 0$ and t [4]

The second neutron, detected at t can either be a "random" neutron (from some other chain) or a chain related neutron. The probability of detecting a random neutron is $A\Delta$, where A is the average counting rate of the detector and Δ is the time interval of measurement. In case the second neutron is a chain related neutron, the probability to detect this neutron after the first, decreases exponentially in time with the prompt neutron decay constant according to $e^{-\alpha t}$. Hence the total probability of detecting a neutron, either random or chain related, in time interval Δ is according to [4]

$$p(t)\Delta = A\Delta + Be^{-\alpha t}\Delta \tag{2.13}$$
$$\text{with } A = F\varepsilon \text{ and } B = \frac{\varepsilon D_v k_p^2}{2(1-k_p)l}$$

Where F is the average fission rate of the system, ε is the detector efficiency in counts per fission, D_v is the so called Diven parameter, that is an appropriate normalized average for the number of prompt neutrons per fission, k_p is the prompt multiplication factor (i.e. neglecting the delayed neutrons), and l is the neutron lifetime.

The derivation of this equation will be disregarded, but noteworthy is that $A\Delta$ represents the background due to uncorrelated counts. When $A\Delta$ can be removed, a single exponential term is left, from which the decay constant α can be evaluated. A depends on the fission rate, while B, the chain related term, is independent of the power level. Lowering the fission rate will increase the signal-to-noise ratio of the measurements.

By plotting the probability density $p(t)$ obtained experimentally, the prompt neutron decay constant can be found from the correlated part through fitting an exponential function.

2.3.2 Feynman Alpha

In a nuclear reactor, the counts, c, of a neutron detector will deviate from a true Poisson distribution due to the presence of fissile material. By relating the variance to mean of the number of counts collected in a fixed time interval, to this time interval, alpha can be determined. This statistical method is called the Feynman technique [4]. Feynman used the Rossi method to define that the variance to mean ratio could be given as a function of alpha and the time intervals used in the measurements.

$$\frac{\overline{s^2}}{\overline{c}} = \frac{\overline{c^2} - \overline{c}^2}{\overline{c}} = 1 + \frac{\varepsilon D_v}{\rho_p^2}\left(1 - \frac{1-e^{-\alpha T}}{\alpha T}\right)$$
$$\frac{\overline{c^2} - \overline{c}^2}{\overline{c}} - 1 = Y \tag{2.14}$$
$$\text{where } Y = \frac{\varepsilon D_v}{\rho_p^2}\left(1 - \frac{1-e^{-\alpha T}}{\alpha T}\right)$$

This derivation is done by considering the number of combinations of two events out of a set of events within time interval *ΔT*. See for more details [4]

Alpha can be found by measuring the variance to mean ratio for fixed time intervals and fitting *Y* in these measurement results. This fitting will be done for two variables, alpha and *g*,

where *g* represents $\frac{\varepsilon D_v}{\rho_p^2}$.

Therefore *g* depends on the detector efficiency, Diven's parameter and the reactivity of the prompt neutrons. Although the detector efficiency is a constant, it can vary slightly from one measurement to the other.

Because the measured value always consists of a summation of the different alpha modes, a new Feynman alpha formula for an arbitrary number of alpha modes was derived [5].

It has the following form:

$$\mathrm{Y}(\Delta\mathrm{T})=\mathrm{C}_0\sum_{k=0}^{N-1}\sum_{l=0}^{N-1}C_{k,l}\frac{1}{\alpha_k\alpha_l}\left[1+\frac{\alpha_l^2(1-e^{\alpha_k\Delta T})+\alpha_k^2(1-e^{\alpha_l\Delta T})}{\alpha_k\alpha_l(\alpha_k+\alpha_l)\Delta T}\right] \tag{2.15}$$

Where *C* with index of subscript are constants, and N is the number of alpha-modes taken into account. It should be noted that in this formula the sign convention of α has been conserved.

Previous research on the alpha modes in Delphi [6], considered only the first two modes of equation 2.14 and by redefining the coefficients obtained the following more convenient expression.

$$\mathrm{Y}(\mathrm{T})=\mathrm{c}_0\cdot\left(1-\frac{1-e^{-\alpha_0 T}}{\alpha_0\cdot T}\right)+\mathrm{c}_1\cdot\left(1-\frac{1-e^{-\alpha_1 T}}{\alpha_1\cdot T}\right) \tag{2.16}$$

2.4 Delphi subcritical assembly.

For educational and research purposes the TU Delft is equipped with a zero power subcritical reactor. For safety reasons this reactor is located in the reactor hall, next to the HOR, a 2 MW thermal reactor for higher education and research. Delphi is a small reactor in which the fuel rods can be manually controlled. An accurate description of the reactor geometry is important for the calculations of the alpha modes. A report about Delphi [7] gives the following description:

Figure 1. Delphi subcritical assembly [7]

The Delphi assembly contains 168 fuel pins, each of which contains 43 to 45 pellets made of 3.8% enriched UO_2 fuel. The pellets are stacked in an aluminium tube with outer diameter of 12 mm and wall thickness of 0.95 mm. Each pellet has an outer diameter of 5.05 mm and a height of 10 mm. Each pin has a length of 69.5 cm; from bottom to top a fuel pin contains 5 cm of aluminium, 6 cm of corundum, 44 cm or 43 cm of fuel, 3 cm of corundum, 3.15 cm of void (spring), 5 cm aluminium and a stainless steel head to facilitate grabbing by a special handling tool. The fuel pins are positioned in a square lattice of 13x13, with the central position being occupied by a water filled tube. The pitch between the fuel pins is 23 mm. The core is placed in the middle of a cylindrical stainless steel vessel with both an inner diameter and height of 100 cm and a wall thickness of 3 mm. The vessel is filled with de-mineralized water until about 5 cm below the top of the vessel. The ^{252}Cf-neutron source contained in a plastic capsule has an initial strength of 18.5MBq (October 2003) corresponding to a neutron source emission rate of 2.4 10^6 s^{-1} and a gamma-ray emission rate of 1.3 10^7 s^{-1}. The source is stored in a stainless steel box and can be inserted to the bottom of the fuel pins by air pressure. The energy spectrum of the neutrons from the source can be found in appendix 1.

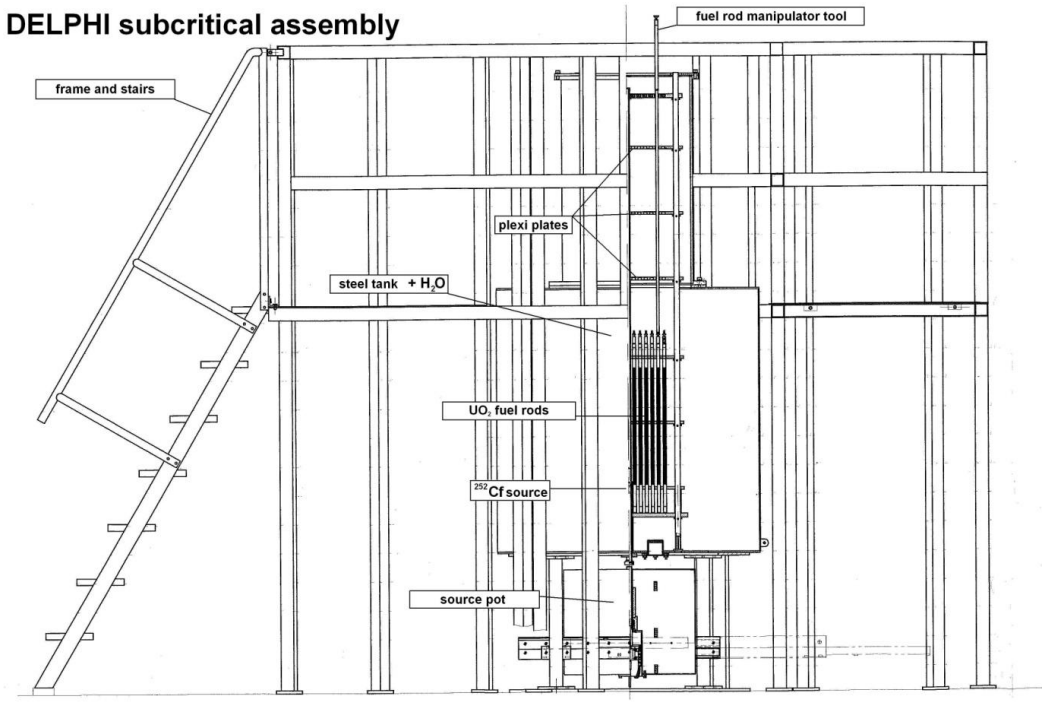

Figure 2. Scheme of the Delphi subcritical assembly [6]

3. Alpha mode calculations

In this chapter it is explained how the alpha modes were calculated. It focus on what steps are taken to determine accurate alpha values, and it describes what programs have been used and what assumptions have been made.

3.1 Determining alpha

Transients inside a sub critical reactor can be analyzed analytically by solving the time-dependent neutron diffusion equation directly. Because the equation has five degrees of freedom, energy, time and space this problem is difficult to solve. To get an idea of the order of magnitude of the alpha eigenvalue, an analytical calculation has been made [8]. To keep the calculation simple, only two energy groups have been used and only the fundamental and the first higher order alpha are determined.[1] For this analytical determination of the alpha, cross sections and the neutron speed are necessary to execute the calculation. Therefore the same cross sections and the neutron speed have been used as for solving the problem numerically. These values were obtained with SCALE [9]. A more detailed description of this process will follow in the next section.

Because such a calculation is not accurate, the eigenvalue problem will be solved numerically. For that purpose the DALTON code is used. This code is based on direct discretization of the neutron diffusion equation, which is deterministic, in time, energy and space. The energy dependence is introduced through the multi-group approach. [2].

3.2 Basic principles of DALTON

The DALTON code [10] is able to solve the 3D multi-group diffusion equations on structured grids (*xyz* or *rzϑ* coordinates). The code calculates both the fundamental and higher order modes and uses the Implicitly Restarted Arnoldi Method (IRAM). This is a method to solve eigenvalue problems, and was used several times to find the effective multiplication factor, k_{eff} , of a multiplying system, which is the dominant eigenvalue of the set of λ-eigenvalues. The IRAM is freely available in the ARPACK package [11]. For generating accurate values, the input needs to be an accurate description of the subcritical assembly Delphi. Besides the geometry, the energy groups and the corresponding cross sections have to be determined.

3.3 Cross sections generation

The cross sections are dependent of the geometry of the reactor and the energy of the neutrons. To generate the cross sections for several energy groups the SCALE package has been used. First some simplifications in the geometry have been made to make the calculation less complex.

With SCALE the cross-sections for two zones have been obtained. The fuel pins and the water in the core were homogenized as one zone, the moderator as a second zone.

To calculate the cross sections in the fuel pin, some simplifications have been made. The pins were simplified as if they were only made of fuel and an aluminium cladding, neglecting the corundum and the spring in the pins, (fig 3.) For the same reason the fuel amount in each pin is assumed to be the same, neglecting the fact that some pins contain 43 pellets while other contain 45 pellets UO_2.

[1] Henceforth, the fundamental alpha will be referred to as 'one' and the first higher order alpha will be referred to as 'two'.

Furthermore the cross sections in the fuel pins were computed, by homogenizing the simplified fuel pins and the surrounding water as a whole (fig. 4). The dimensions of the square surrounding the fuel pin correspond to the pitch between two pins. To generate the cross sections for the complete reactor core another simplification was made. In total there are 168 pins, in a square lattice, 13 x 13 positions, with the central position being occupied by a water-filled tube. In the SCALE calculations this hole in the central position is neglected, and assumed to be filled with a fuel pin as well. This assumption causes the model to calculate cross sections based on more fuel than there actually is. As this is only 1/168, this will not significantly influence the calculation. The second zone for which SCALE generated the cross sections is the moderator.

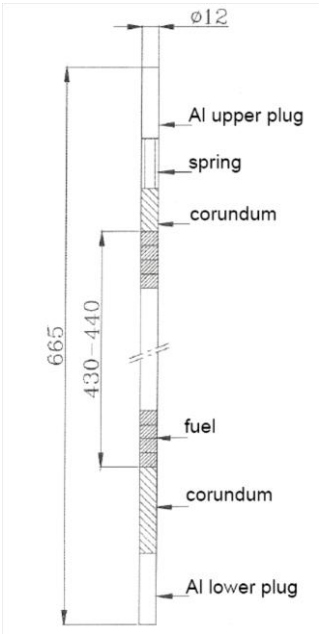

Figure 3. Fuel pin schematic

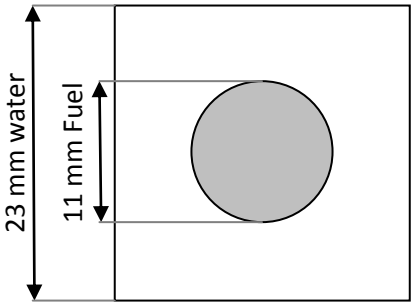

Figure 4. Schematic view of a fuel pin from above. The water surrounding the fuel and the fuel are homogenized as one zone in SCALE

After determining the homogenized fuel as one zone, and the moderator as the other, the various energy groups have to be collapsed. This causes the reaction rate to be constant, in order to speed up the calculation. The XSDRN module of SCALE [12] calculates this reaction rate by a volume integral of the flux times the cross sections, in an integral over different groups. The neutrons have to be divided into groups first. Since neutrons usually lose energy during their lifetime a backward indexing scheme is used for the numbering of the energy groups. The group with the highest number corresponds with the neutrons with the lowest energy. In XSDRN 238 energy groups with fixed boundaries are given. To keep the calculation simple, the number of groups was reduced. To set the boundaries and determine the amount of groups various energy group structures were used and the results of k_{eff} have been compared. The final group classification is based on the k_{eff} with the slightest deviation compared to the value of k_{eff} after convergence by calculations with 20 and 50 energy groups. For 10 groups, the calculation has been made with several different energy boundaries, called a, b and c. The same is done for 20 groups (a-b). The K_{eff} results of the number of groups with specified energy boundaries are shown in table 1. The corresponding boundaries for the energy groups can be found in appendix 2.

Table 1. The multiplication factor K_{eff} for different energy group structures.

Number of energy groups	K_{eff}
10 a	0.934800
10 b	0.951246
10 c	0.943893
12	0.951607
20 a	0.953138
20 b	0.950854
50	0.953669

As shown in table 1, the result for 12 groups has the slightest deviation compared to the results for 50 energy groups. The difference between 10 (b) and 12 groups is very small and there is no expectation of measuring more than two alpha's, it was decided to use only ten groups.

The distribution of the neutrons on the groups that are used is shown in table 2.

Table 2. Distribution of the energy variable over 10 energy groups

Group	Energy range
1	0.92 MeV- 20 MeV
2	850 keV – 0.92 MeV
3	9.5 keV – 850 keV
4	950 eV- 9.5 keV
5	90 eV – 950 eV
6	9.1 eV – 90 eV
7	975 meV – 9.1 eV
8	90 meV – 975 meV
9	7.5 meV – 90 meV
10	10 µeV- 7.5 meV

The input data used for the generation of the cross sections in SCALE can be found in appendix 3.

The cross sections belonging to the 10 energy groups and the two homogenized zones are stored in a library, which has been used in the DALTON calculations. This library contains twenty different kinds of cross sections for each zone, of which eight are relevant for the alpha mode calculations. Given the multi group diffusion equation the important cross sections are the fission cross section, the scatter cross section, the total cross section and, because the diffusion coefficient depends on this, the transmission cross section. In the SCALE library these cross sections can be found as the absorption cross section, the neutron transport based on outscatter approximation, the neutron transport based on inscatter approximation, fission cross section, the elastic, nonelastic and inelastic collision cross sections.

3.4 The grid used for the DALTON calculations

DALTON solves the diffusion equation on given points in the reactor. Therefore a model was created, based on the geometry of Delphi. The more accurate the geometry, the more expensive the

calculation is. Therefore some simplifications have been made compared to reality. The reactor is located in a cylindrical vessel (fig. 5), but in DALTON the moderator zone is programmed as if it was a rectangular vessel. This assumption will not significantly influence the results of the calculations because the neutrons will not reach the edge of the reactor. This is plausible because the reactor is safe to stand next to. It is made sure that there are hardly any neutrons outside the wall.

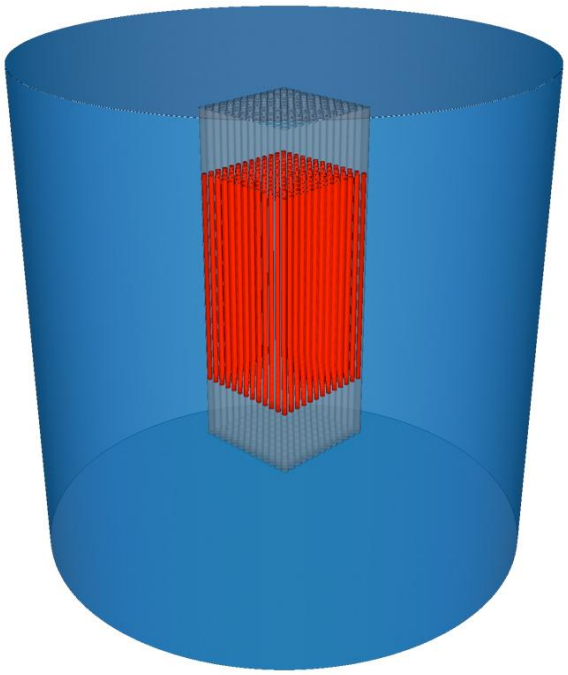

Figure 5. Schematic view of the realistic situation in Delphi

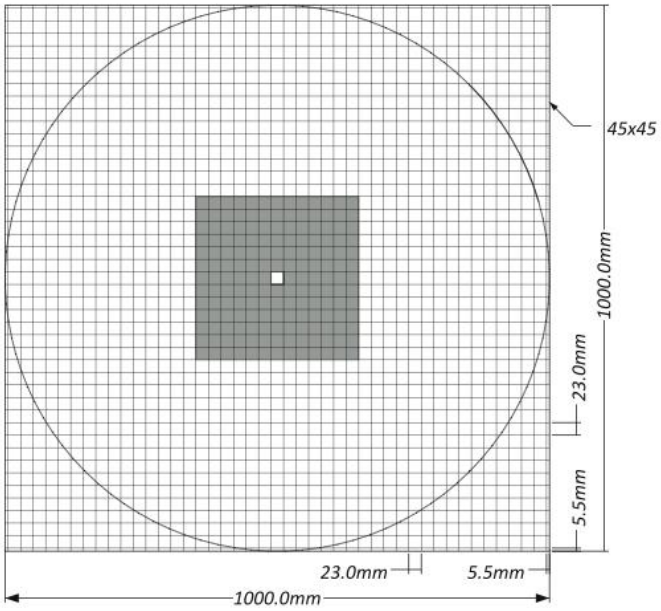

Figure 6. Schematic representation of the XY-plane of the grid used for DALTON calculations

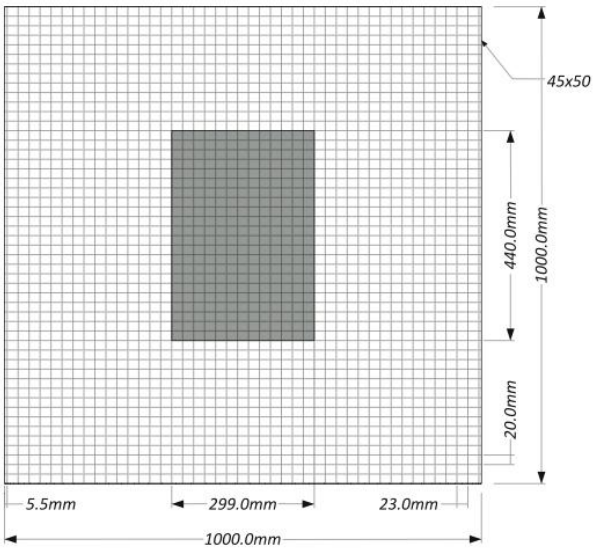

Figure 7. Schematic representation of the XZ-plane

The grid in DALTON contains 101250 volumes (45x45x50). The grid is chosen in such a way that the cells in DALTON coincide with the homogenized fuel rods. The structured XYZ-grids are plotted in the XY-plane and XZ-plane in figure 6 and 7, where the grey cells contain the fuel and the white cells contain the moderator. In the figure it can be seen that in the center position of the XY -plane itself is a cell with moderator. In reality, the center is also a tube filled with water, as at that spot the external source is introduced at the bottom of the vessel. The calculation is performed twice, once with the geometry as shown in the figure, and once with the middle position filled with fuel. The first calculation corresponds to the real situation. The reason for the second calculation is that these results will better correspond to the results of the analytical calculations, since these were performed with the assumption the fuel zone was uniform.

For the calculation vacuum boundary conditions are used.

4. Mode measurements

The alpha mode gives the rate at which the associated flux-shape decays in the absence of a source. It is therefore possible to measure alpha in a zero power reactor with several noise techniques. These techniques are based on detecting neutrons that originate from the same fission chain. In large power reactors many fission chains occur simultaneously, making it unlikely that detected neutrons correlate to each other in space and time.

This section explains how the measurements are done, describes the materials used and elaborate the detector positioning. It concludes with a description of the desired measurements.

4.1 Instrumentation

The neutron detectors used for this research are 10-bar ^{3}He proportional counter tubes with a diameter of 6 mm and an active length of 76 mm. The pulses from the detector are amplified and converted to TTL format (standardized 'square box' pulses with a height of 5 V) by PDT amplifiers (PDT20A-SHV), which also supplies the high voltage.

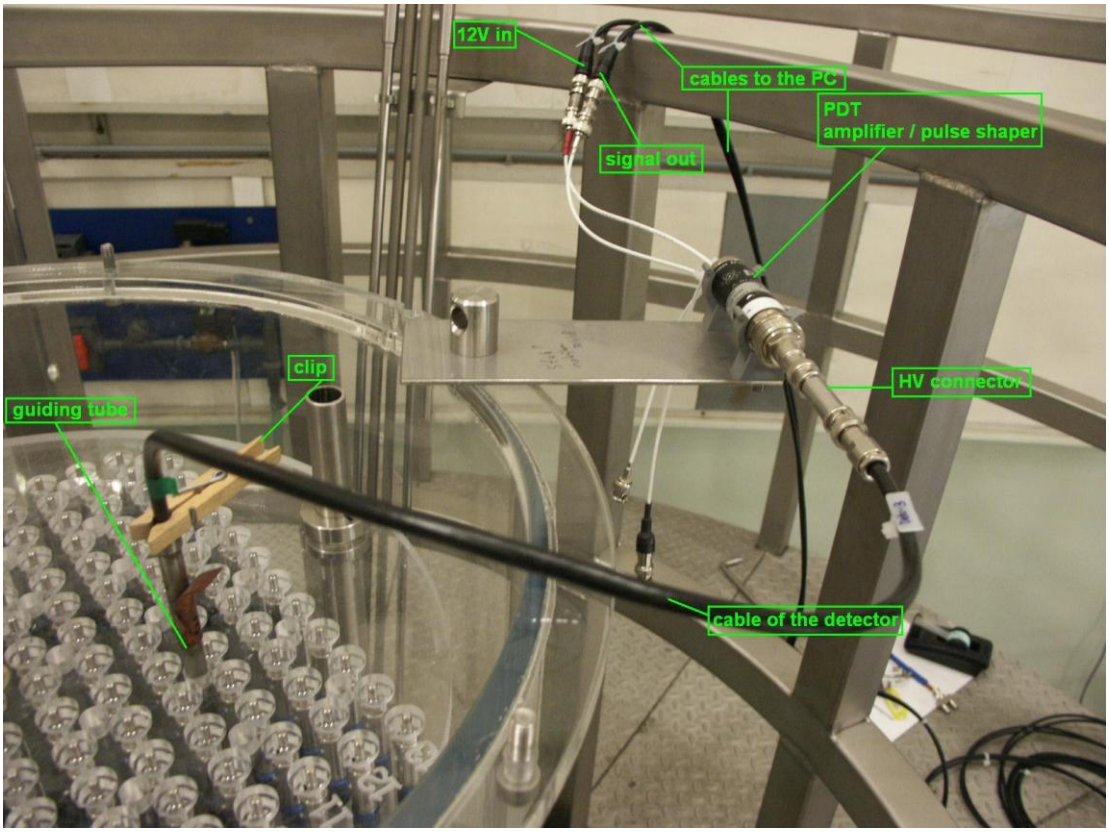

Figure 8. Layout of the instruments [6]

The pulses are subsequently recorded on a PC equipped with a pulse-counter card and LabView software to control the measurements. To determine the alpha value from the measurements a program is used, developed by a student of Budapest University of Technology and Economics, Institute of Nuclear Techniques. This program measures and registers the time intervals between the

peaks of the signal that the counter card receives, using the own time base of the card, which is 20MHz as a sampler. It repeatedly determines the variance-to-mean ratio at a given time interval. The time interval ranges from 1 µs to 10 ms.

To interpret the results form LabVIEW, a program [13] is used to convert the data from labview to the variance to mean ratio per time interval.

The variance-to-mean ratio can be plotted against the width of the time intervals and the alpha value can be determined by fitting Y within the measurement results.

$$Y = \frac{\varepsilon D_v}{\rho_p^{\,2}}\left(1 - \frac{1 - e^{-\alpha T}}{\alpha T}\right) \tag{4.1}$$

Prior to this, the data must be processed, since Y is not equal to the variance to mean, but to the variance to the mean minus one (eq. 2.12). After fitting Y, the residual of the data should be plotted, to see if multiple alpha-modes can be identified.

4.2 Detector positions

The detectors can be placed in the reactor by putting tubes between the fuel rods. Besides the holes for the fuel rods there are 36 holes in the grid for possible positions for the detectors. The vertical distance of the detectors with respect to the middle of the fuel rods can be chosen freely, by putting the detector deeper or more shallow into the tube.

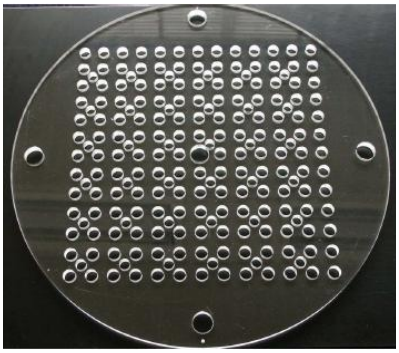

Figure 9. One of the acrylic grid plates with diameter of 425 mm. Between the holes for the fuel pins (13x13-1=168 positions), smaller holes for the detector tube can be seen. [7]

To increase the possibility of good measurement results the detector positioning is important. The results of measurements will always be contaminated since at the same time several modes will be measured. The most important mode to measure is the fundamental alpha mode. This describes the flux shape at which the flux will decay and the rate at which the decay proceeds. Since this mode continues to exist for the longest period, only this fundamental mode is of importance in determining the reactivity. The fundamental alpha mode also gives the alpha that is expected to be measured, since higher modes will always decay faster. On the other hand, the fact that other modes extinguish faster, does not mean they are not measured. On the contrary, the alpha expected to measure will always be contaminated by the other existing flux forms. Therefore it is important to place the detectors on a position where the fundamental mode is dominant with respect to all other modes. On this spot the measurement will be the least polluted.

It is therefore interesting to take a closer look at the flux shape corresponding to various alpha modes. Since it is not possible to measure the flux shape, it is necessary to study the calculated flux shape. This is done for all modes at several contour levels in different energy groups. The shape of the flux can be shown in a mid XY plane, or with a contour level in a XYZ figure.

The next series of graphs shows the shape of the flux in different energy groups in the entire reactor. The graphs show the shape of the flux with contour levels at 0.001 (Green), -0.0001 (red), 0.0002 (yellow) and -0.0002 (blue).

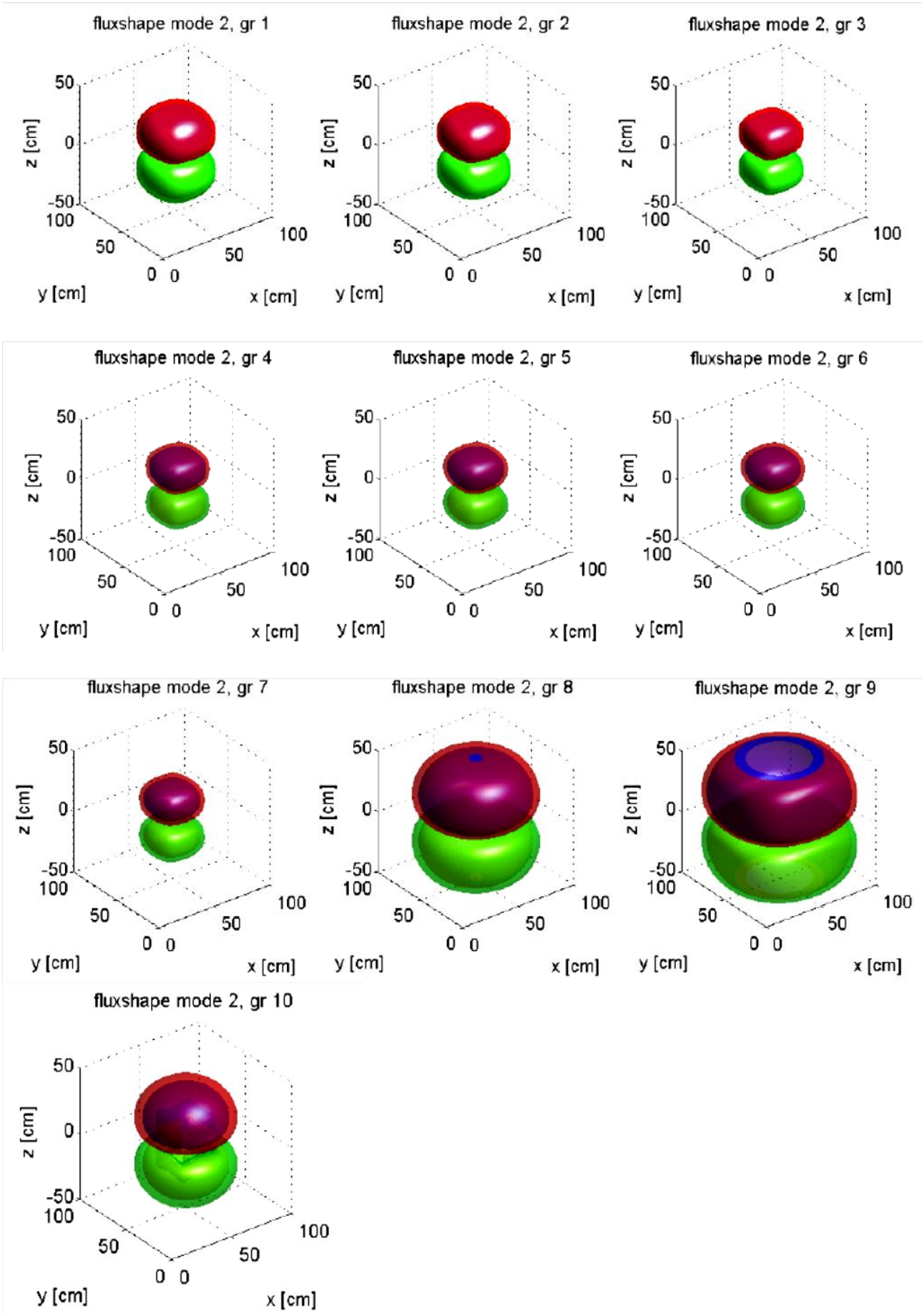

Figure 10. The flux shape for mode 2 for all energy groups

In figure 10 it is clear that the contours of the flux are not exactly the same for different energy groups. At the same time it shows that the different energy groups do not cause much difference in the shape of the flux. The shape will more or less stay two spheroids upon each other, only the size varies. In energy group ten, the position of the fuel zone is visible.

To show how the flux shape vary in different modes, the next series of graphs demonstrate the flux shapes of the fundamental mode, and mode 3, 5, 7, 8, 9 and 10 for three energy groups. The contour levels are the same as for the second mode: 0.001 (Green), -0.0001 (red), 0.0002 (yellow) and -0.0002 (blue).

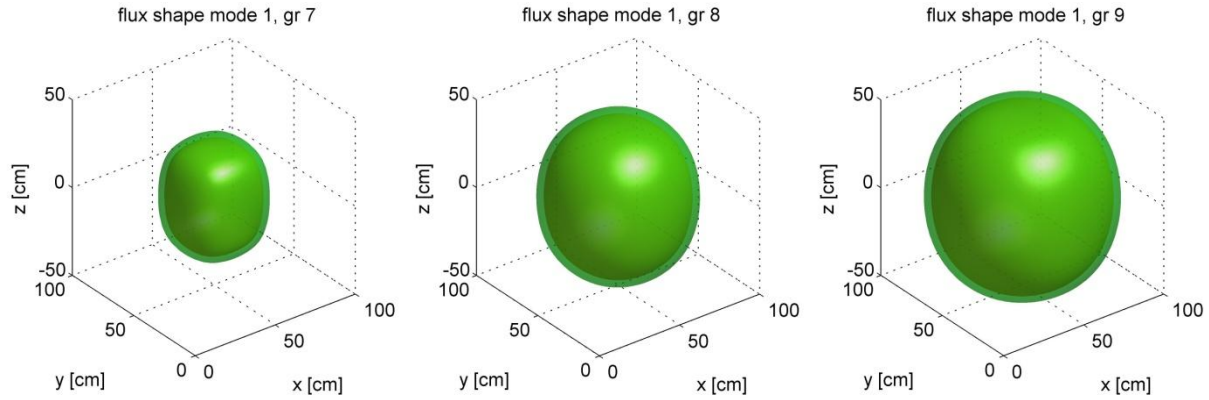

Figure 11. Contour levels of the flux shape in the fundamental mode

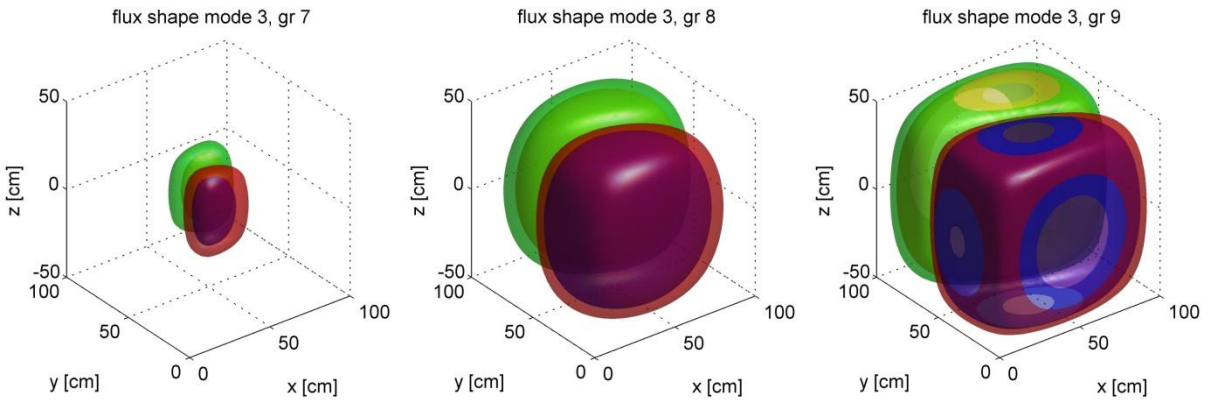

Figure 12. Contour levels of the flux shape in the 3th mode

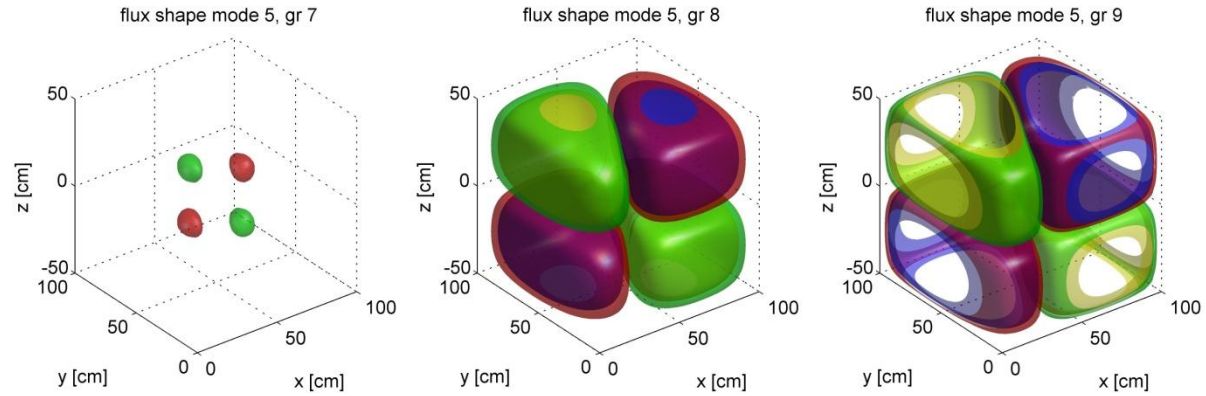

Figure 13. Contour levels of the flux shape in the 5th mode

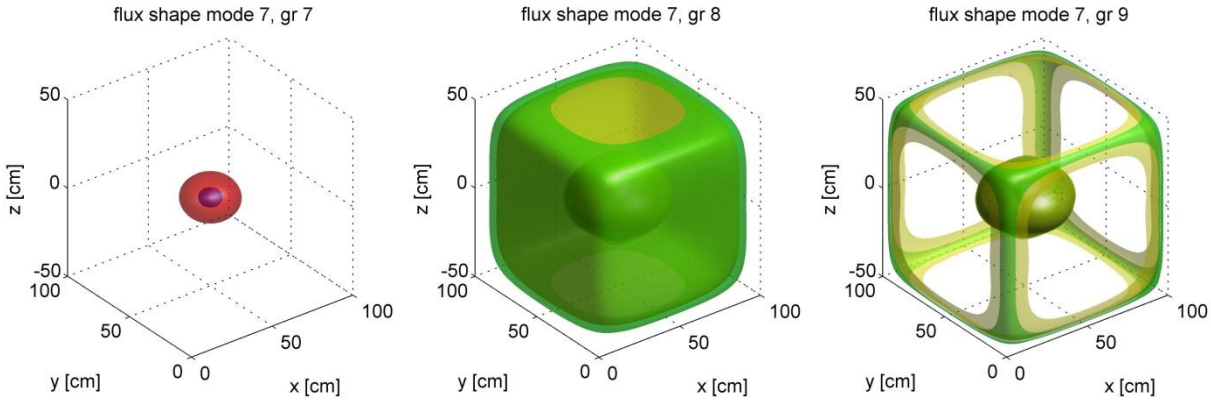

Figure 14. Contour levels of the flux shape in the 7th mode

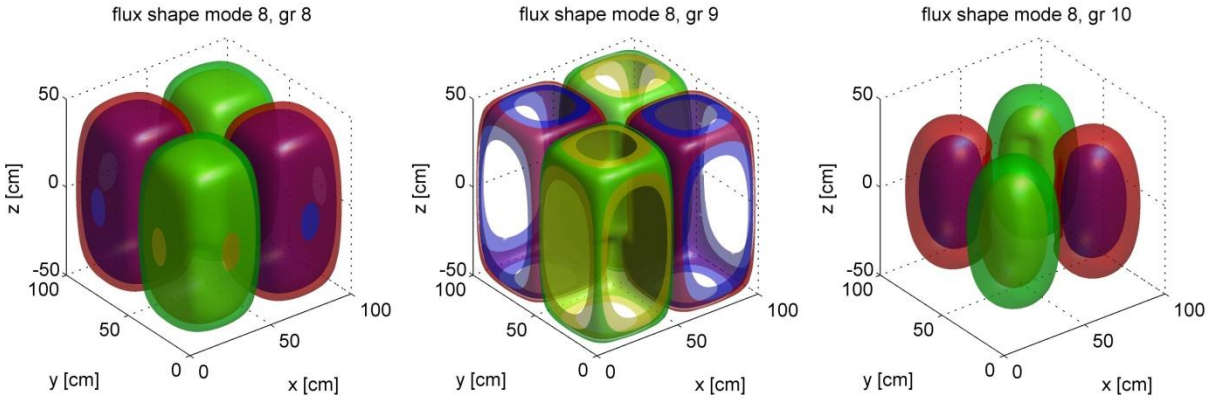

Figure 15. Contour levels of the flux shape in the 8th mode

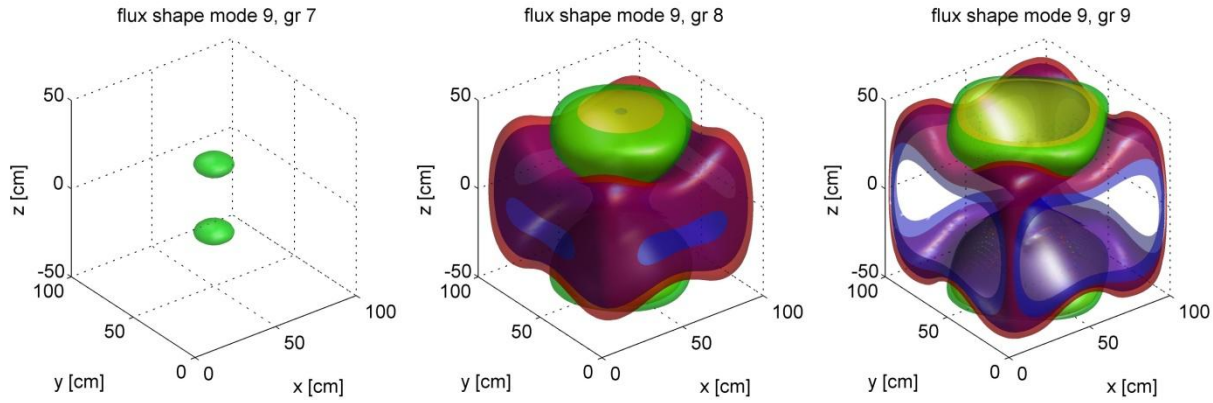

Figure 16. Contour levels of the flux shape in the 9th mode

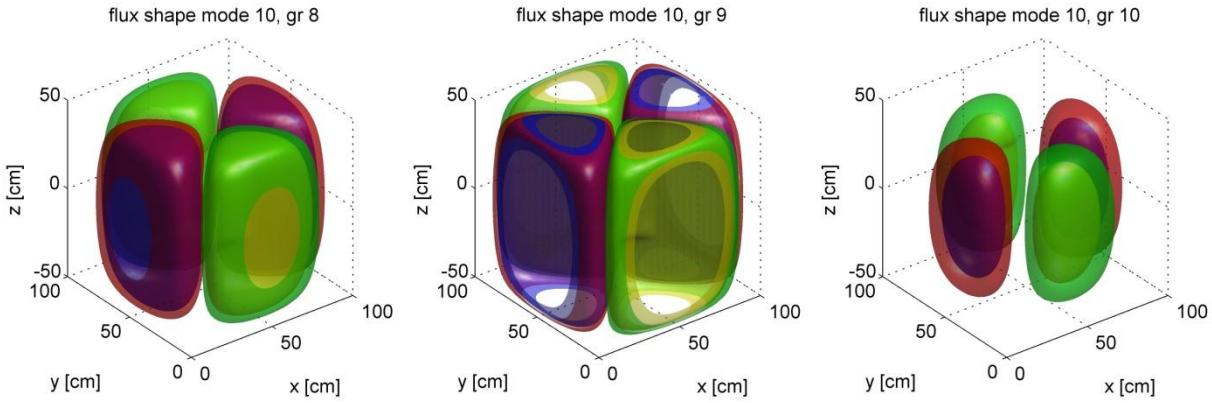

Figure 17. Contour levels of the flux shape in the 10th mode

These figures show that the flux shape strongly differs in different modes and to a lesser extent in different energy groups. These graphs are made with four different contour plots.

In order to determine where the detectors should be placed, it is important to know at which places the fundamental mode has the highest value, and at which places the higher order modes have a absolute minimum value. The zero contours of the higher order modes are plotted in graphs. This is done for all energy groups. To show that the minimum depends on the mode and not that much on the energy group the minima for energy group 2 and 8 for all modes are plotted in figures 18 and 19.

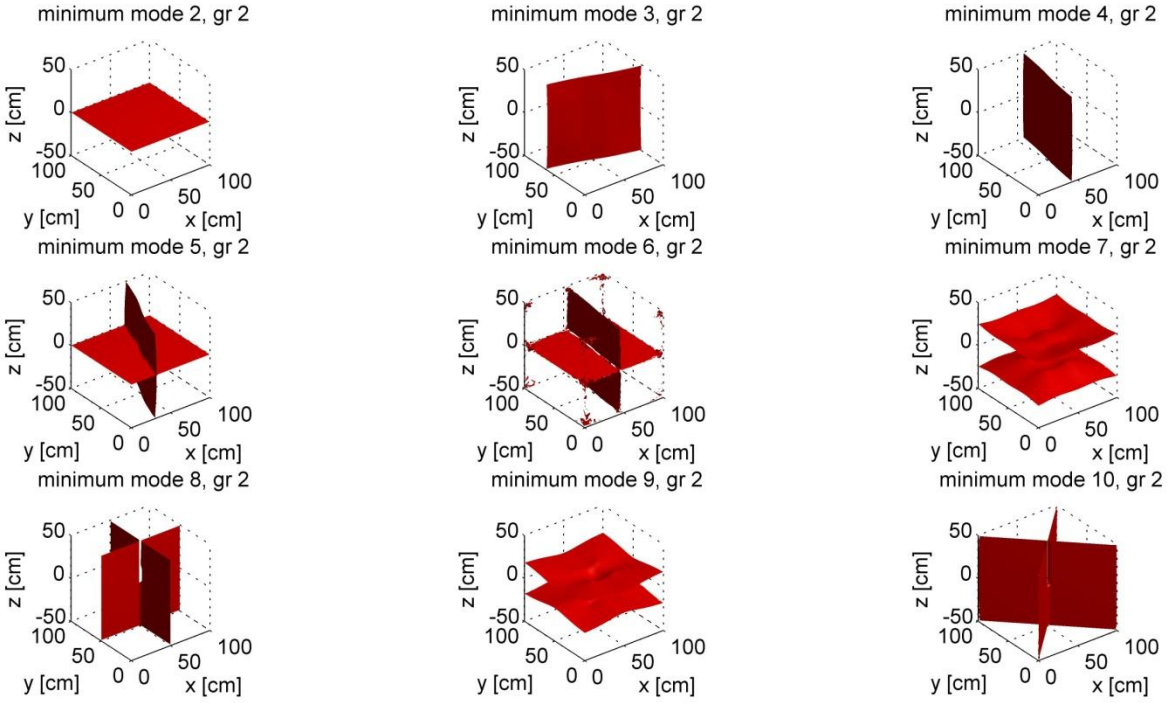

Figure 18. Minima of the 2nd group for all modes

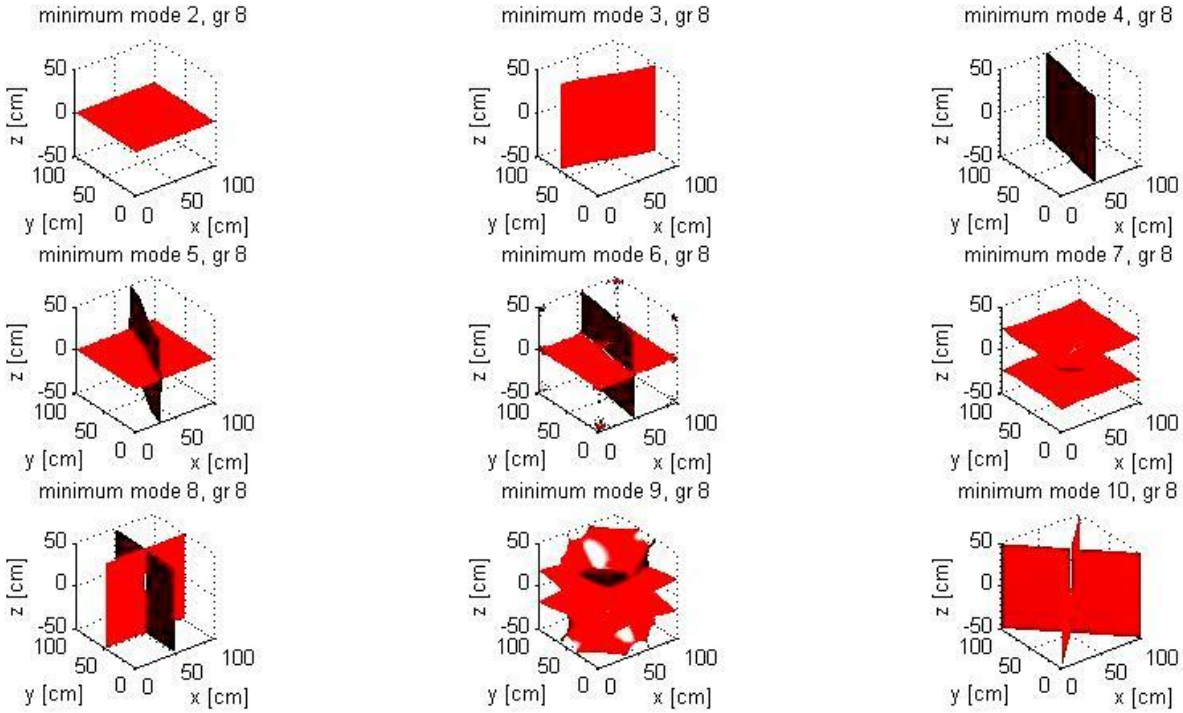

Figure 19. Minima of the 8th group for all modes

Since multiple alpha modes per energy group are expected, a summation of all absolute minima are plotted together in one graph. This is done for every energy group, figures 20 and 21 show the result for group 2 and group 8.

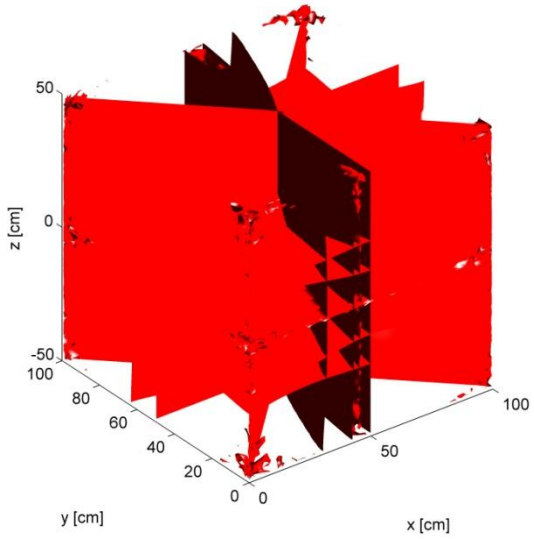

Figure 20. Energy group 2, minimum values mode 2-10

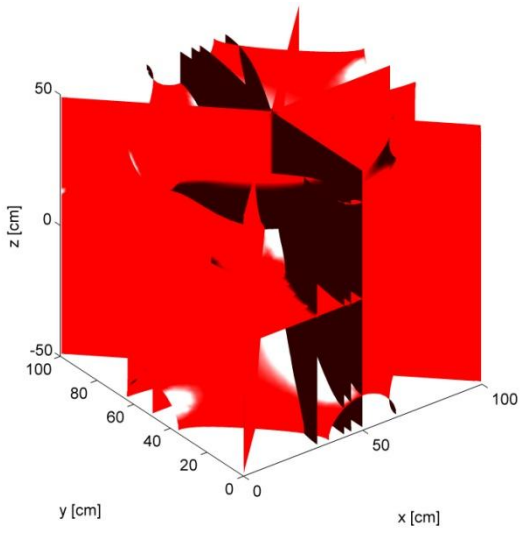

Figure 21. Energy group 8, minimum values mode 2-10

These figures make clear that there is not a single position where all modes have a minimum value. Figure 18. and 19. showed clearly that mode 7 and 9 do not have a minimum at the middle of the reactor core, where all other modes do have a minimum.
In order to determine the optimal detector position, a short Matlab script (appendix 4) has been used. It uses the results of the DALTON calculations and computes for every possible detector position the following:

$$a = \frac{|\phi_1|}{\sum_{\alpha=1}^{10} |\phi_\alpha|} \tag{4.2}$$

The absolute flux value of fundamental alpha mode at all possible detector positions was divided by the sum of the absolute value of flux values of all modes at that position. The position with the highest value is likely to be adequate for the detector, because of the biggest difference between the fundamental mode and the other modes. The lowest value indicates the most undesirable detector position.

This calculation is done for each energy group. The program gives the coordinates of the most adequate position and a graphic image of the values at all positions. Figure 22 shows a isometric projection of the results for detector positions for the first energy group, followed by cross-sections in the XZ and XY plane.

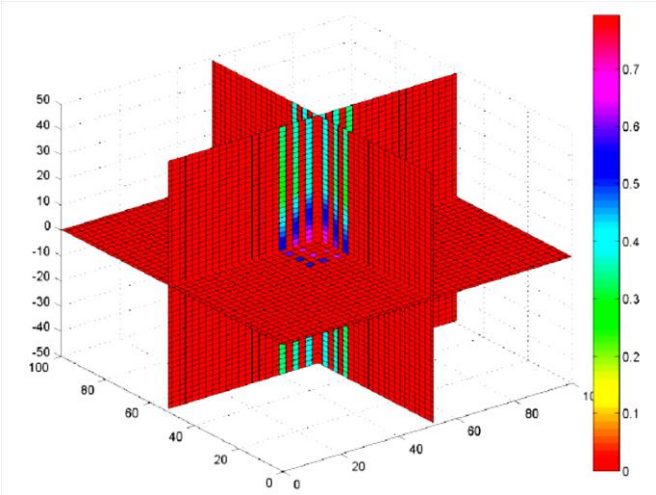

Figure 22. The result of Matlab for the most suitable detector positions

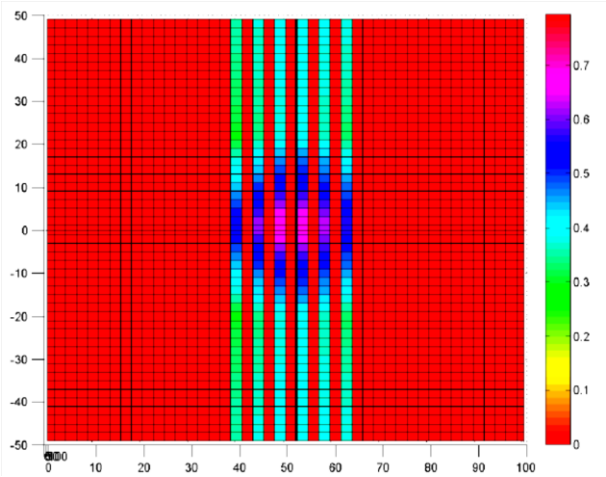

Figure 23. The results for detector positions for the first energy group in the XZ plane.

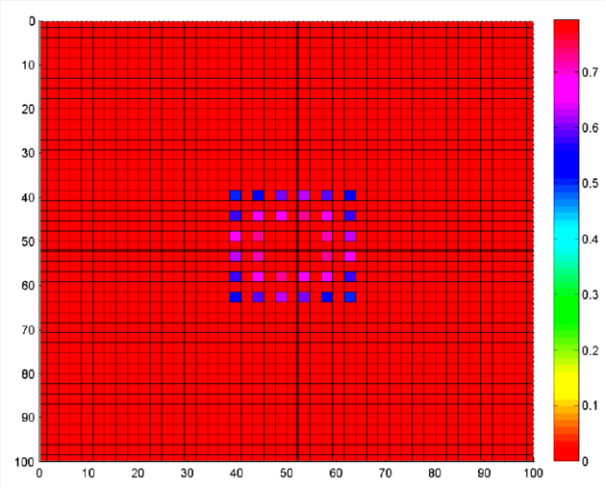

Figure 24. The result for detector positions for the first energy group in the XY plane

However this method takes into account the time in which a flux shape extinguish and the maximal difference between the fundamental mode and the higher modes, it does not take into account the expansion coefficient, which is physically the amplitude of the flux shape (eq. 2.12). To achieve all the information out of the measurement results this information is essential. Unfortunately, there is no information available about the amplitude, only that it depends on the shape of the initial flux. Although this method ignores the value of this expansion coefficient, it might as well give a good indication of the potentially suitable position for the detectors, since the amplitude has no effect if the flux is zero.

The XY coordinates that Matlab returns as result of the above calculations, correspond to the most central position as the potentially suitable position and the outer position as the least favorable position. The final measurement positions are shown schematically in Figure 20. The most beneficial position is H-I 6-7, with a height of 22 cm from the bottom of the fuel zone. This depth corresponds with the middle of the fuel zone. The least favorable position shows to be L-M, 12-13, with a height of 44 cm from the bottom of the fuel zone, that corresponds with the top of the fuel zone.

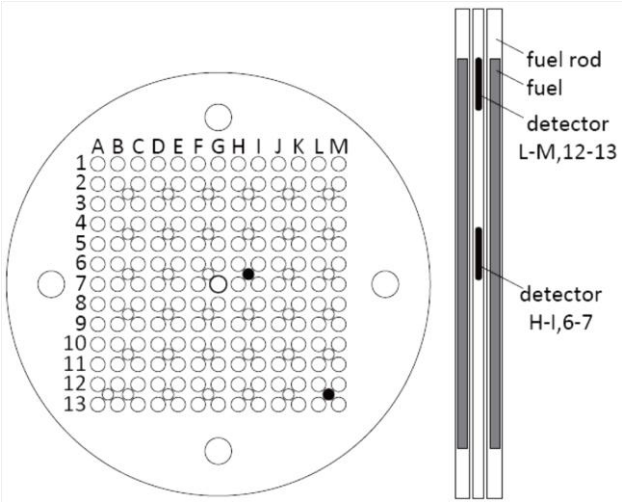

Figure 25. Detector positions and measurement markings

4.3 Dead time correction and error

The program used, determines the variance-to-mean ratio at a given time interval. The variance-to-mean ratio is plotted against the time intervals and alpha is determined by fitting Y within the measurement results (eq. 4.1).

The dead time of the data acquisition system affects the variance-to-mean ratio. Therefore a dead time correction had been applied. This correction is derived from [6]. The dead time correction is applied in the same way as in the work of Klujber. The programs made for this purpose have been used. The derivation of this correction will be disregarded in this thesis.

The accuracy of the fit is determined by the sum of squares due to error (SSE) and the root mean squared error (RMSE). The sum of squares error measures the total deviation of the response values from the fit to the response values.

$$SSE = \sum_{i=1}^{n} w_i (y_i - \hat{y}_i)^2 \tag{4.3}$$

A value closer to 0 indicates that the model has a smaller random error component, and that the fit will be more useful for prediction.

The root mean squared error is an estimate of the standard deviation of the random component in the data, and is defined as

$$RMSE = s = \sqrt{MSE} \tag{4.4}$$

where MSE is the mean square error

$$MSE = \frac{SSE}{v} \tag{4.5}$$

Just as with SSE, RMSE value closer to 0 indicates a fit that is more useful.

In addition to the accuracy of the fit, the accuracy of alpha is determined. This is done by defining two boundaries in which alpha must fall within a level of certainty of 95%. These so called confidence bounds define the lower and upper values of the associated interval. The width of the interval indicates how uncertain the fitted coefficient is

5. Results

During the first period of this research alpha was determined computationally. By the results obtained with DALTON, the most favorable detector position is determined. After that, four measurements are taken, each with two detectors used simultaneously. This chapter gives the results of both the calculations and the measurements and the interpretations of these results. This chapter concludes with the comparison between the measurement results and the calculated alpha's.

5.1 Computational results

Prior to calculating the alpha eigenvalue, the calculated flux shape corresponding to the external neutron source is visualized, to gain insight in the simulated situation. After that, the DALTON calculations is performed several times. In the next sections the raw and edited data are presented for 20 and 30 modes calculations. The symmetry of several modes will be discussed and finally the multiplication factor corresponding to the calculated alpha eigenvalue is given.

Results of the DALTON calculation with neutron source.

DALTON is also able to run the program for a reactor with an external neutron source. This was done by implementing the neutron source information in DALTON. DALTON calculates the flux shape corresponding to this source. Some contour levels are plotted to visualize the flux shape.

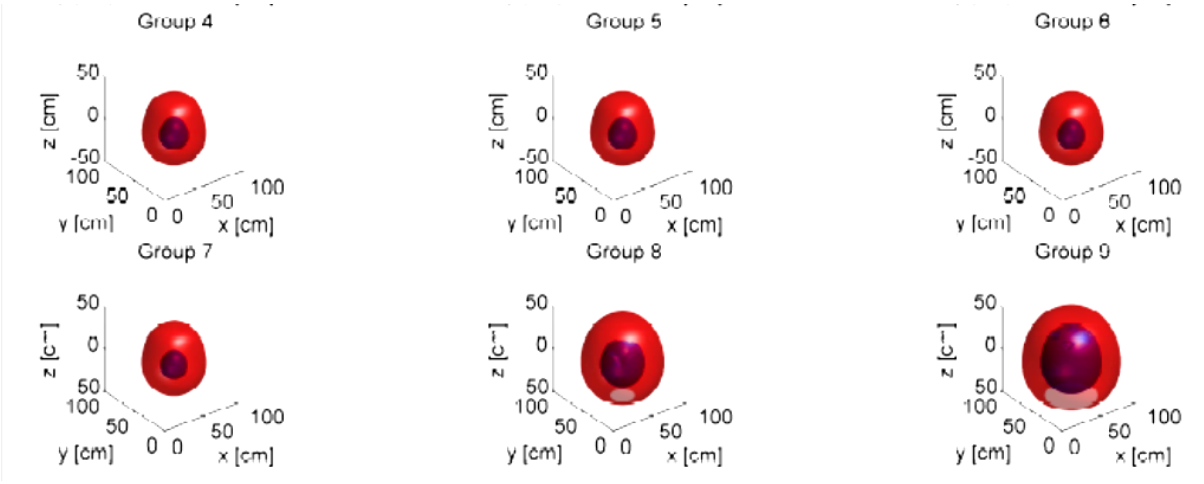

Figure 30. Contour levels show the flux shape of the external neutron source

Multiple alpha modes

Table 3 gives the eigenvalues of twenty alpha modes, calculated by DALTON for ten energy groups.

Table 3. Alpha eigenvalues of 20 modes

#	Alpha eigenvalue	#	Alpha eigenvalue
1	-2332.630264	11	-5484.350777
2	-4673.303174	12	-5475.42756
3	-5150.255521	13	-5475.427772
4	-5150.252463	14	-5553.369145
5	-2046512.229	15	-5600.861593
6	-116169.9612	16	-5646.480964
7	-41267.95603	17	-5648.946814
8	-22297.0234	18	-5673.033746
9	-13156.81811	19	-5673.035766
10	-5514.837119	20	-5721.868712

The first thing that strikes is that the eigenvalues are not decreasing. They were expected to decrease, since the Arnoldi method claims to search for successive eigenvalues. With this insight, it can be concluded that it is not certain whether there were eigenvalues in between the values given by DALTON. Another thing that can be noticed is that the values from number 5 till 9 significantly vary from the other eigenvalues. It is plausible these eigenvalues belong to a higher mode than the first twenty.

The results from the calculations with 30 modes (table 4.) confirm this expectation. These results are also not decreasing, but are afterwards sorted from largest to smallest. The highest absolute value, 5980.199151, is much lower than the absolute value of numbers 5 till 9 in the 20 modes calculation. It is strange that there are values in the 20 modes calculations that are not calculated in the 30 modes calculations. This and the fact that the results are not sorted as expected, implies an artifact in ARPACK, since the input data regardless the number of modes, does not differ.

Table 4. Alpha eigenvalues of 30 modes

mode	Alpha eigenvalue	mode	Alpha eigenvalue	Mode	Alpha eigenvalue
1	-2332.630264	11	-5646.480503	21	-5821.233478
2	-4673.303174	12	-5648.945858	22	-5832.980436
3	-5150.252453	13	-5673.033744	23	-5841.942217
4	-5150.255521	14	-5673.03589	24	-5885.750376
5	-5475.42756	15	-5719.002548	25	-5895.709963
6	-5475.427939	16	-5719.003887	26	-5906.231697
7	-5484.350588	17	-5721.868558	27	-5948.959822
8	-5514.837127	18	-5817.852848	28	-5949.211349
9	-5553.369106	19	-5817.853451	23	-5972.196798
10	-5600.861576	20	-5821.231171	30	-5980.199151

A closer look at this table shows that many eigenvalues (within the deviation of 6.0 10^{-5}%) are present in duplicate. For example alpha of the third and fourth mode and alpha of the fifth and sixth

mode. This can be explained by orthogonality relations of the alpha modes. [14] [15]. This is caused by the symmetry of the reactor geometry. Because of the symmetry of the reactor there may be similar flux shapes with a opposite sign, or a rotation. These flux shapes extinguish simultaneously, and thus have the same corresponding time eigenvalue. DALTON also gives the eigenvectors corresponding to the calculated eigenvalues. These represent the associated flux shape. By making some contour levels visible, the flux shapes show this symmetry very clearly. Figure 26 and 27 show several contour levels of the flux shape of the third and fourth mode. The shape of the modes are similar, but a rotation has occurred. Figure 28 and 29 show that the shape of the fifth mode is similar to the shape of the sixth mode, but with opposite sign.

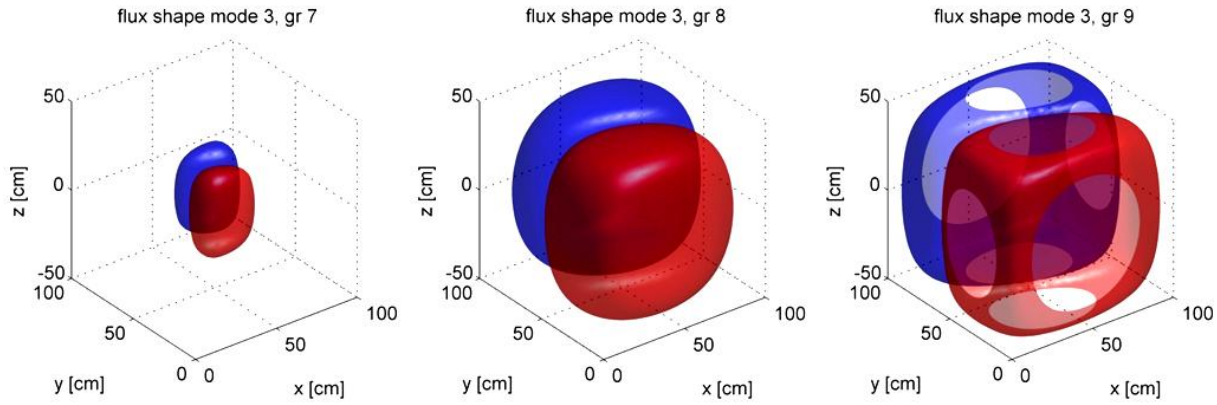

Figure 26 Flux shape of mode 3. (0.0001 blue, -0.001 red)

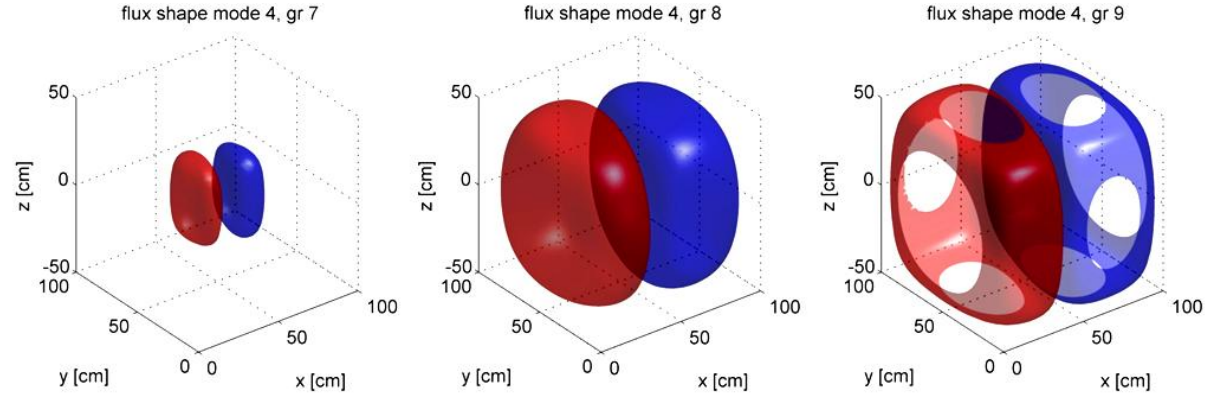

Figure 27 Flux shape of mode 4. (0.0001 blue, -0.001 red)

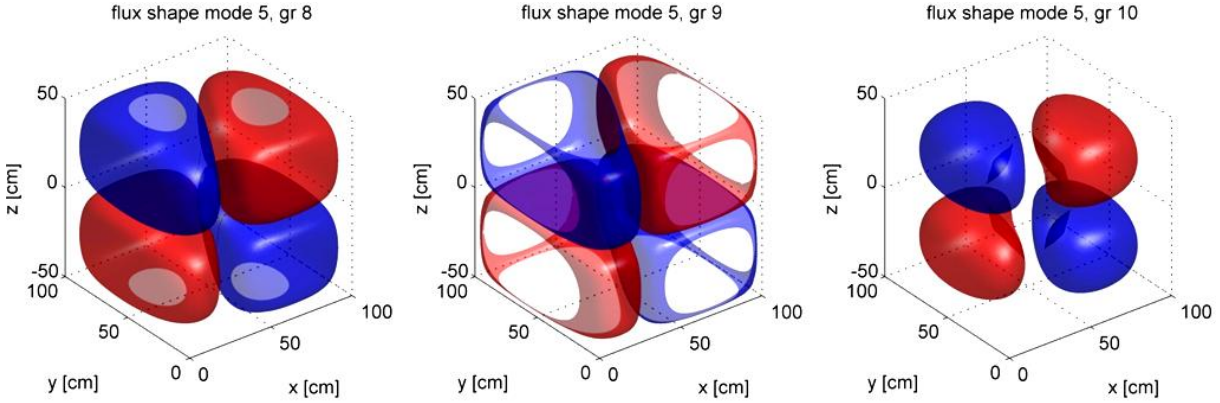

Figure 28 Flux shape of mode 5. (0.0001 blue, -0.001 red)

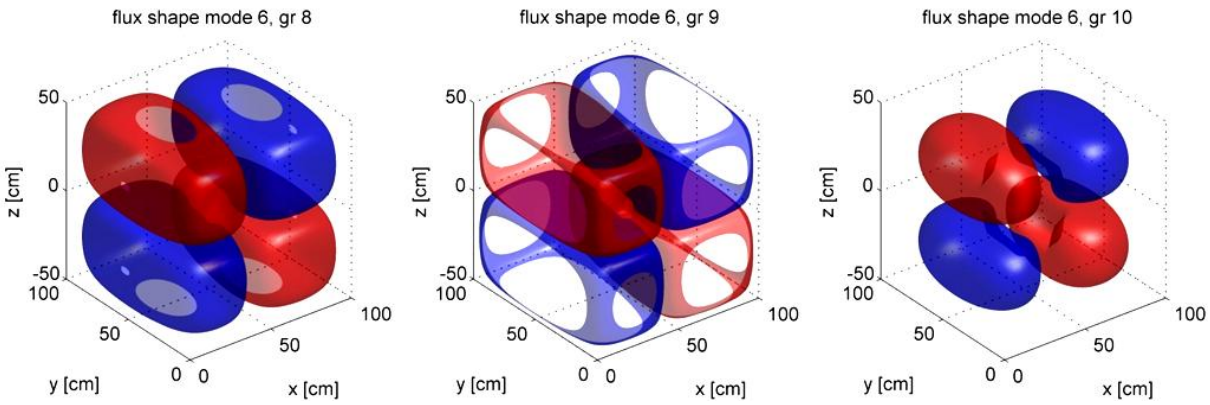

Figure 29. Flux shape of mode 6. (0.0001 blue, -0.001 red)

The results of the calculation for ten modes corresponds to the first ten eigenvalues of the previous calculation. The eigenvalues of the higher order alpha modes do not differ very much, that makes it unlikely to measure multiple higher modes. The small difference means that they will extinguish about the same time. So if one of the higher alpha modes is present, then others will be present as well. The eigenvalue of the fundamental mode varies significantly from that one's belonging to the next alpha modes. If these values match reality, it would be possible to measure the fundamental alpha mode and a mixture of the higher alpha modes.

With a slightly different input, but with the same reactor geometry, the DALTON code is able to calculate the multiplication factor. The k_{eff} that corresponds to the input that gives an alpha of -2332 is 0,85892.

5.2 Results of noise measurements

In order to determine alpha by measurements, two detectors are used simultaneously. The positions of the detectors are determined in section 4.2. Because different detectors may have different detector efficiency, there was a variation in the use of the detectors.

The table below gives information about the used detectors, the measurement positions, the measurement duration, and date.

Table 5. Overview measurements information

Name	Date	Measurement time (h)	Position	Detector	Amplifier	Counter
110712D1	6-12-11	4	F-G, 6-7, 22 cm	2		1
110712D2	6-12-11	4	L-M, 12-13, 44 cm	1		2
120419M1D1	4-19-12	3	I-H, 6-7 22 cm	3	3	1
120419M1D2	4-19-12	3	L-M, 12-13 44 cm	2	4	2
120419M2D1	4-19-12	1.5	I-H, 6-7 22 cm	3	3	1
120419M2D2	4-19-12	1.5	L-M, 12-13 44 cm	2	4	2
120426D1	4-26-12	3	L-M, 12-13 44 cm	3	3	1
120426D2	4-26-12	3	I-H, 6-7 22 cm	2	4	2

The results of the measurements are plotted in a graph, and fitted to determine alpha. Because of the possible occurrence of multiple alpha-modes, two fits have been applied to the data. After fitting data, the goodness of fit was evaluated. The term goodness of fit is used in several senses. [16] A good fit is a model in which coefficients can be estimated with little uncertainty, or a model that explains the variability in the data, and is able to predict new observations with high certainty.

A visual examination of the fitted curve is a first step, and the residual analysis a second. The residuals from a fitted model are defined as the differences between the response data and the fit to the response data at each predictor value.

Assuming the fitted model to the data is correct, the residuals approximate the random errors. Therefore, if the residuals appear to behave randomly, it suggests that the model fits the data well. However, if the residuals display a systematic pattern, it is a clear sign that the model fits the data poorly.

In figure 30 and 31 fittings of one and two alpha modes to Feynman-alpha data are displayed. It gives not a clear result that more than one alpha is measured.

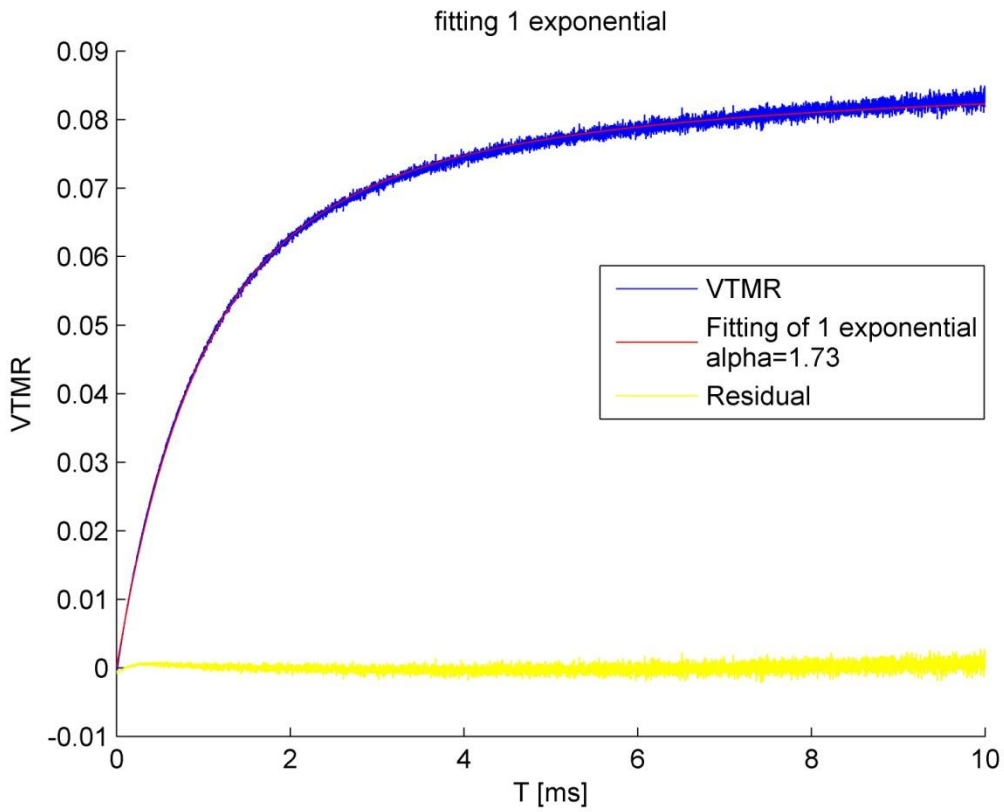

Figure 30. The variance to mean ratio with fitting curve with one alpha

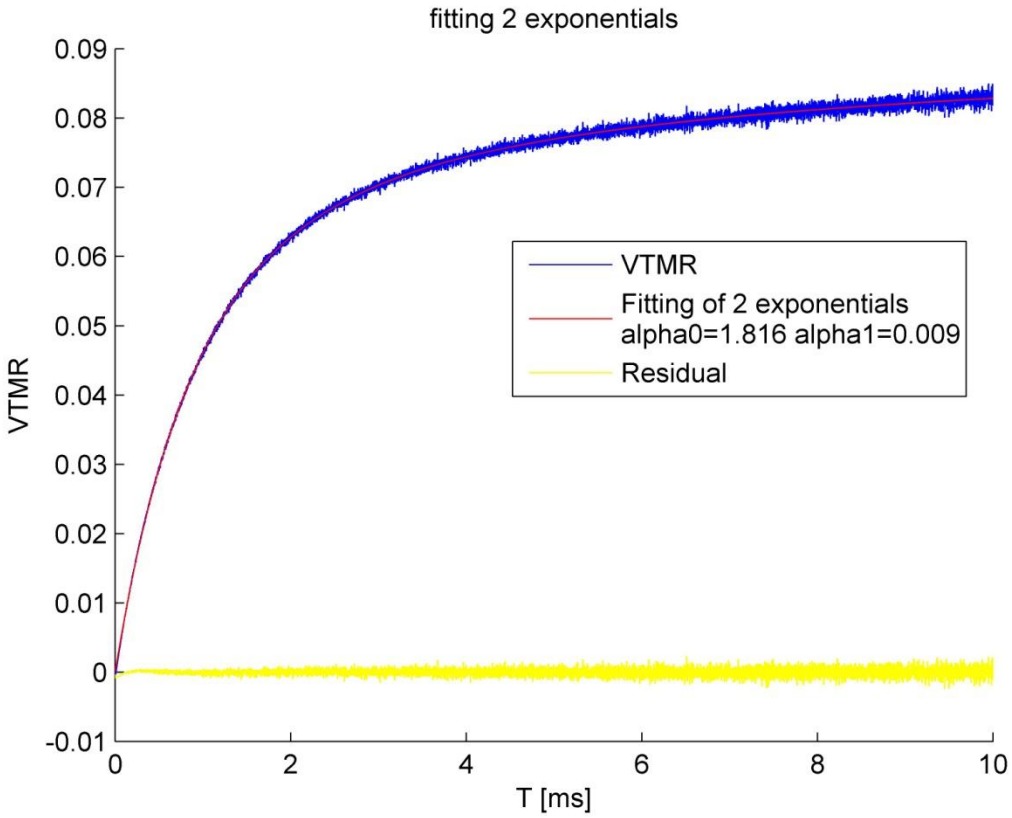

Figure 31. The variance to mean ratio with fitting curve with one alpha

The residuals appear randomly scattered around zero, indicating that the model describes the data well. At very small gate widths, a small peak can be observed. With the two-exponentials residual this peak still exists, thus the need of a second alpha is not confirmed with this visual analysis.

Most of the graphs look similar, and therefore are not shown. However, one measurement failed. The figure below shows the result of this measurement. The measurement will be disregarded.

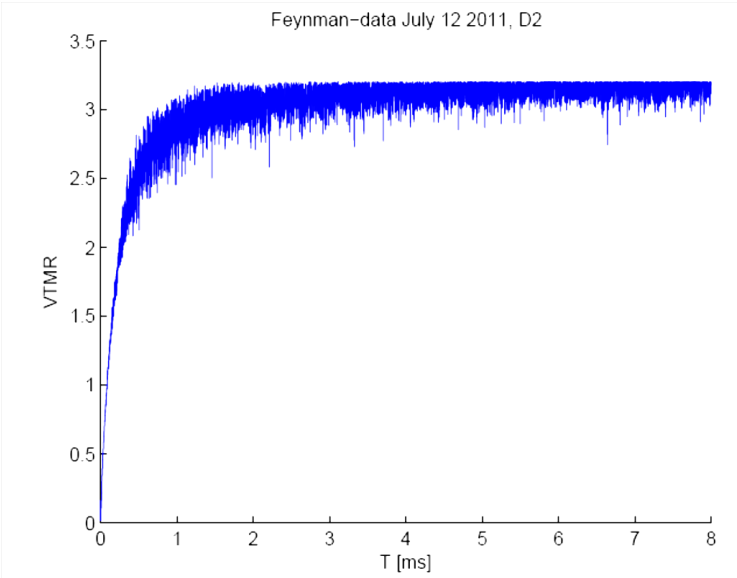

Figure 32. Data of failed measurement July 2011

The graphs and the plotted residual give limited information, therefore the goodness of fit should be examined by statistics. This is done by calculating the sum of squares due to error (SSE) and the root mean squared error (RMSE).

Table 6. Results for fundamental and first higher alpha eigenvalue after fits in feynman data April 19.

120419M2D2	Alpha		C		SSE	RMSE
Fit 1 exponential	1.544		0.02417		0.007007	0.0008372
Fit 2 exponentials	0.003367	1.635	0.04912	0.0234	0.006928	0.0008325

Before further conclusions can be drawn two reservations must be observed. Matlab indicates a positive value for the alpha as a result of the requested function. These values should be interpreted as a negative number. Secondly, Matlab gives alpha with unit [ms^{-1}]. This means that alpha should be multiplied by 1000 in order to obtain alpha [s^{-1}].

The results for the measurement of April 19 (table 6.) show that the error in the fit with two exponentials not significantly decreased. Besides that, the time eigenvalue belonging to the first higher alpha mode should in absolute value be increased. This is not the case with this, and other measurements. The results after fitting a second exponential gives in all cases a lower absolute value than the fundamental alpha, and can therefore be regarded as invalid.

Table 7. Results for alpha after fits in Feynman data.

	Position	Alpha (with 95% confidence interval)	C	SSE	RMSE
110712D1	F-G, 6-7, 22 cm	1.73 [1.728, 1.732]	0.0873	0.003455	0.0005879
120419M1D1	I-H, 6-7 22 cm	2.027 [2.006, 2.047]	0.0703	0.1234	0.003513
120419M1D2	L-M, 12-13 44 cm	1.797 [1.788, 1.807]	0.0218	0.003366	0.0005802
120419M2D1	I-H, 6-7 22 cm	1.803 [1.798, 1.808]	0.06927	0.01085	0.001042
120419M2D2	L-M, 12-13 44 cm	1.544 [1.533, 1.554]	0.02417	0.007007	0.0008372
120426D1	L-M, 12-13 44 cm	2.079 [2.067, 2.09]	0.02119	0.003449	0.0005873
120426D2	I-H, 6-7 22 cm	1.802 [1.799, 1.806]	0.06902	0.004172	0.000646

The measurement results of April 26 correspond to the expectations with regard to the detector positioning. The expectation was that the detector in the middle was most likely to measure the fundamental mode, as the fundamental mode was expected to be dominant at that position. The detector in the middle position has a lower alpha than the detector positioned at L-M. This is consistent with the expectations, since higher alpha modes will extinguish faster, and have therefore a (absolute) higher time eigenvalue. However, the results of April 19 conflict with this expectation, as the values in the middle position are higher than the values at the, as expected, less favourable position.

This might be caused by the amplitudes of the 7th and 9th mode. It is possible that the amplitudes of modes 7 and 9 were bigger during the measurements of April 19, in comparison to the measurements of April 26. This can be explained by the fact that the amplitude depends on the initial condition. The initial conditions are related to how the source is introduced. It is likely that the

results of various measurements on April 19 was not substantially different, given the initial conditions for both measurements have been the same. The source is not removed between measurements. It can also be explained that the initial conditions at April 26 differ from those on April 19, and it would therefore be explained that the amplitudes during the measurements of April 19 differ from the amplitudes during the measurement of April 26. That is why these measurements are not necessarily in contradiction with each other. A comment should be made that not only the seventh and the ninth mode with corresponding amplitudes can influence the measurement. The calculation for the detector position is created by using data of only ten modes. In reality, many more modes are present. If there are twenty modes with a similar time decay constant, and from the thirty mode calculations it is known that they exist, then these twenty flux shapes also affect the measured values, while that is not included in the determination of the detector position.

Never the less, there is still that the measurements do not necessarily contradict. On the other hand it can be said that the introduction of the source should not differ significantly as it is a quick process. Therefore the question arises whether it is possible that a small variation in the initial condition can cause a wide variation in the amplitude and thus the flux. In other words, is the problem stable or instable?

Apart from this question can be concluded that the fundamental alpha will have in magnitude a lower value, and thus a relatively higher value, than the measured alphas. This is because there can be assumed that there is always measured a mix of multiple alpha modes. The higher order alpha modes have a relatively lower time eigenvalue. So without these higher modes, the fundamental alpha is relatively higher than the measured alpha.

Another conclusion that can be drawn is that there are too less measurement results to exclude if measurements are in contradiction with each other or with expectations. From the measurement on July 12, data of the second detector is missing. The other two measurements do not provide enough information to draw conclusions based on the corresponding results.

5.3 Comparing measurement and computational results

In summary, the following results do occur, in which the measured values were converted to comparable units.

Table 8. Summarized results for alpha

	DALTON calculations	Measurements
Fundamental α	-2332	[-2079, -1544]
α_2	-4673	
α_3	-5150	
k_{eff}	0.85892	0.92

The measured alpha eigenvalues are difficult to compare with the calculated eigenvalues, given the large differences between the measured eigenvalues relative to the calculated ones. Thereby it is not known to what extent the fundamental mode is measured and how much influence the higher modes have. The comparison becomes easier when the corresponding multiplication factor is

involved in the comparison. The k_{eff} which belongs to the DALTON calculations is 0.85892. About the actual k_{eff}, limited information is available. When Delphi in 2003 was put in service, the maximum k_{eff} was 0.92. For this comparison, 0.86 and 0.92 will be used, knowing that these are not exact.

As concluded in section 5.2, the real value of the fundamental time eigenvalue is a relatively higher value, than the measured alphas. This strikes with the expectation looking at the relation between the multiplication factor and the time eigenvalues. A lower multiplication factor indicates a lower time decay constant. The measured alpha should at least be higher than -2332, since DALTON has to do with a lower multiplication factor. This can be mathematically supported by the following equation. Neglecting the delayed neutrons, [4] gives

$$\alpha = \frac{1 - k_{eff}}{l} \tag{5.1}$$

with l the neutron lifetime.

Assuming the neutron lifetime is in both cases similar, which is not the case since l depends on k_{eff} a first-order approximation of alpha can be made.

$$\frac{1 - k_{eff,D}}{\alpha_D} = \frac{1 - k_{eff,m}}{\alpha_m}$$

where α_D represents alpha determined with DALTON and α_m the measured alpha.

$$\frac{1 - 0.84}{-2332} = \frac{1 - 0.92}{\alpha_m}$$

This equation returns -1666 for α_m. The measured values do not exclude the existence of a fundamental mode with a time decay constant of -1666 s^{-1}. On the other hand, the measured results do also not exclude that the k_{eff} meanwhile became lower than 0.92.

Apart from the fact that assumptions are made that are not physically correct, does the comparison of the measured and calculated alphas not exclude that the results match. These results do not call for the assumption that the measurements and calculations contradict each other. However it also does not guarantee the accuracy of both the measurements and the calculations. Further research is acquired.

6. Conclusions and Recommendations

6.1 Conclusions

The main purpose of this research was to make a global comparison between the calculated and measured alpha modes of subcritical assembly Delphi. To this end in the first period of the research alpha was determined computationally.

There are several assumptions concerning the reactor geometry. After that, cross sections are generated and energy groups are made. DALTON returned 0.85892 as k_{eff}, this was lower than expected, given that Delphi had a k_{eff} of 0.92 when it was built.

The alpha eigenvalues calculated by DALTON make clear that a lot of the higher order alpha eigenvalues are very close together. Some are even present in duplicate. For mode 3 and 4 and for mode 5 and 6, this is the case. The flux forms associated with these modes are visualized, and this shows that or a rotation or symmetry occurs in the corresponding flux shape.

By visualizing the flux shapes of other modes it has become clear that the flux shape is strongly determined by the mode, and to a lesser extent by the energy of the neutrons. Within all visualisations of the flux shape, the amplitude corresponding to the alpha mode is not taken into account, since there is no information available about this amplitude. Nevertheless, this amplitude can make a significant difference in reality.

A last conclusion that can be drawn after computing the alpha modes with DALTON is that the eigenvalues are not sorted when returned. This implies an artefact in APRACK.

With the calculated flux shapes, a calculation is performed to determine the optimal detector position. With respect to the minima of the different flux shapes, often a flat surface crossing the center of the reactor, it was not remarkable that the ideal detector position seemed to be the middle of the reactor core.

Subsequently, measurements were made. One measurement failed, other measured values appear to contradict each other, but this could be explained on the basis of the amplitudes depending on initial conditions. Unfortunately too few measurements are made to draw a valid conclusion. Besides that there was too much variation in the constants. For example, measurements were taken with different detectors, on different locations, with different initial conditions and for varying measurement periods. The maximal measurement period was four hours, but the results of this measurement was not significant better than the result of shorter measurements.

Finally a general comparison between the measured and calculated results was made. The conclusion that follows was expected, given the different values for k_{eff}. The k_{eff} in the DALTON calculations was lower than the assumed k_{eff} for Delphi, so the alpha eigenvalue of the calculations was lower than the measured alpha eigenvalue.

It is difficult to draw further conclusions from this data, since there is no accurate data of the k_{eff} of Delphi available and since there are too many different measurement results. Moreover, there was not a good insight in what extend the measured value truly exist from the fundamental mode or whether it is contaminated by higher alpha modes.

6.2 Recommendations

As indicated in the conclusions, there is no reason to assume that the measurements and calculations contradict each other. However, to guarantee the accuracy of the measurements and the calculations further research is required.

At first the input and the corresponding multiplication factor of DALTON should be investigated. When it is clear where the unexpectedly low k_{eff} comes from, it can be judged if the simplifications that are made are justified. In addition, it should be investigated what makes that DALTON does not sort the results, and whether this has consequences for producing the correct modes.

Secondly, there are more measurements required. In a series of measurements, the variables like measuring equipment, measurement time and detector positions should be constant to acquire comparable data. It is also recommended to interpret the obtained data in multiple ways. For example with Rossi-alpha measurement techniques or by other techniques described in [1].

Also, a test for the stability of the problem is required, to determine how large the influence of the initial conditions is on the amplitude.

Finally, a good equation is required to relate alpha and the multiplication factor, without making any assumptions which are physically incorrect.

Appendix 1. External Source ^{252}Cf

Table 1.The energy spectrum of the neutron source divided into energy groups.

Energy group in SCALE	Energy (MeV)	Normalized %	Energy group in SCALE	Energy (MeV)	Normalized %
6	1,40E+01	6,94E-05	8	5,50E-01	1,68E-02
6	1,30E+01	1,42E-04	8	5,00E-01	1,66E-02
6	1,20E+01	2,88E-04	8	4,50E-01	1,63E-02
6	1,10E+01	5,83E-04	8	4,00E-01	1,60E-02
6	1,00E+01	1,17E-03	8	3,50E-01	1,55E-02
7	9,00E+00	2,33E-03	8	3,00E-01	1,49E-02
7	8,00E+00	4,61E-03	8	2,50E-01	1,42E-02
7	7,00E+00	9,01E-03	8	2,00E-01	1,33E-02
7	6,00E+00	1,74E-02	8	1,50E-01	1,21E-02
7	5,00E+00	3,30E-02	8	1,00E-01	1,05E-02
7	4,50E+00	2,58E-02	9	8,00E-02	3,68E-03
7	4,00E+00	3,49E-02	9	6,00E-02	3,29E-03
7	3,50E+00	4,68E-02	9	4,00E-02	2,80E-03
7	3,00E+00	6,21E-02	9	2,00E-02	2,17E-03
7	2,60E+00	6,33E-02	9	1,00E-02	7,74E-04
7	2,30E+00	5,67E-02	10	6,00E-03	2,30E-04
7	2,00E+00	6,55E-02	10	3,00E-03	1,28E-04
7	1,80E+00	4,88E-02	10	1,00E-03	5,51E-05
7	1,60E+00	5,31E-02	10	7,00E-04	5,68E-06
7	1,40E+00	5,73E-02	10	4,00E-04	4,53E-06
7	1,20E+00	6,12E-02	10	2,00E-04	2,21E-06
7	1,00E+00	6,46E-02	10	1,00E-04	7,82E-07
8	9,00E-01	3,33E-02	10	5,00E-05	2,76E-07
8	8,00E-01	3,37E-02	10	1,00E-05	1,27E-07
8	7,00E-01	3,39E-02	10	1,00E-06	1,11E-08
8	6,00E-01	3,38E-02	10	4,14E-07	3,10E-10

Appendix 2. Determining energy groups

Energy boundaries and corresponding k_{eff} for determining accurate energy groups.

50 groups					
k_{eff}	**9,54E-01**				
No.		Boundaries	No.		Boundaries
1	10	2,00E+07	26	4	1,35E+00
2	10	4,30E+06	27	4	1,20E+00
3	10	1,20E+06	28	4	1,13E+00
4	10	6,70E+05	29	4	1,09E+00
5	10	2,70E+05	30	4	1,05E+00
6	10	5,20E+04	31	3	1,01E+00
7	10	3,90E+03	32	3	9,50E-01
8	10	9,50E+02	33	3	8,50E-01
9	10	1,86E+02	34	3	7,00E-01
10	8	7,20E+01	35	3	6,00E-01
11	5	4,92E+01	36	3	4,50E-01
12	5	4,24E+01	37	3	3,50E-01
13	5	3,70E+01	38	3	2,75E-01
14	5	3,18E+01	39	3	2,00E-01
15	5	2,25E+01	40	3	1,25E-01
16	5	1,70E+01	41	2	8,00E-02
17	5	1,29E+01	42	2	6,00E-02
18	5	8,10E+00	43	2	4,00E-02
19	5	6,25E+00	44	2	2,53E-02
20	5	4,00E+00	45	2	7,50E-03
21	4	3,00E+00	46	2	4,00E-03
22	4	2,67E+00	47	2	2,50E-03
23	4	2,30E+00	48	2	1,50E-03
24	4	1,94E+00	49	2	1,00E-03
25	4	1,59E+00	50	2	5,00E-04

20 groups A		
k_{eff}	**9.53E-01**	
No.		Boundaries
1	12	2.00E+07
2	12	2.48E+06
3	12	9.00E+05
4	12	4.40E+05
5	12	7.30E+04
6	12	3.90E+03
7	12	6.70E+02
8	12	1.08E+02
9	12	5.20E+01
10	12	3.70E+01
11	12	2.00E+01
12	12	9.10E+00
13	12	3.73E+00
14	12	2.30E+00
15	12	1.35E+00
16	12	1.09E+00
17	12	9.25E-01
18	12	4.00E-01
19	11	1.00E-01
20	11	5.00E-03
		1.00E-05

20 groups B		
k_{eff}	**9.51E-01**	
#		Boundaries
1	20	2.00E+07
2	20	1.20E+06
3	20	2.70E+05
4	20	3.90E+03
5	15	1.86E+02
6	15	5.34E+01
7	15	3.46E+01
8	15	1.51E+01
9	15	5.40E+00
10	15	2.38E+00
11	12	1.25E+00
12	10	1.07E+00
13	10	9.25E-01
14	6	5.00E-01
15	6	3.00E-01
16	5	1.50E-01
17	5	7.00E-02
18	5	2.53E-02
19	5	3.00E-03
20	4	1.00E-03
		1.00E-05

12 groups		
k_{eff}	**9.52E-01**	
No.		Boundaries
1	7	2.00E+07
2	16	8.19E+06
3	22	9.20E+05
4	12	8.50E+04
5	13	9.50E+03
6	16	9.50E+02
7	46	9.00E+01
8	58	9.10E+00
9	27	9.75E-01
10	9	9.00E-02
11	9	7.50E-03
12	3	7.50E-04
13		1.00E-05

10 groups A		
k_{eff}	**9.43E-01**	
No.		Boundaries
1	40	2.00E+07
2	35	2.70E+05
3	35	2.85E+02
4	35	3.46E+01
5	30	3.50E+00
6	25	1.14E+00
7	16	6.00E-01
8	10	1.00E-01
9	8	7.50E-03
10	4	1.00E-03
		1.00E-05

10 groups B		
k_{eff}	**9.51E-01**	
No.		Boundaries
1	23	2.00E+07
2	22	9.20E+05
3	12	8.50E+04
4	13	9.50E+03
5	16	9.50E+02
6	46	9.00E+01
7	58	9.10E+00
8	27	9.75E-01
9	9	9.00E-02
10	12	7.50E-03
		1.00E-05

10 groups C		
k_{eff}	**9.44E-01**	
No.		Boundaries
1	45	2.00E+07
2	12	8.50E+04
3	13	9.50E+03
4	16	9.50E+02
5	46	9.00E+01
6	58	9.10E+00
7	27	9.75E-01
8	9	9.00E-02
9	9	7.50E-03
10	3	7.50E-04
		1.00E-05

Appendix 3. SCALE input

```
=csasi parm=centrm
blablabla-blabla
v7-238
read comp
U-234 1 0 5.2965094E-6 293 END
U-235 1 0 8.5967019E-4 293 END
U-236 1 0 9.3199636E-6 293 END
U-238 1 0 2.1682378E-2 293 END
O-16  1 0 4.5113329E-2 293 END
Al-27 2 0 6.0262622E-2 293 END
H2O  3 1 293 END
end comp
read celldata
latticecell squarepitch
fuelr=0.505 1
cladr=0.6 2
hpitch=1.15 3
cellmix=1111 end
more data adj=0 cof=3 bal=fine icon=cell end more
end celldata
end
=shell
mv ft02f001 $RTNDIR/pin_xs
ln -fs /home/cdokter/test/pin_xs ft04f001
end
=xsdrn
collapsing
0$$ a3 4 a5 3 e
1$$ 2 2 17 1 0 2 2 16 5 1 10 200 e
3$$ 1 e
4$$ 0 10 3 -2 e
5** a7 44 0 0 0.0 10E-3 0.75 T
13$$ 1  2
14$$ 1111 3
15** 1  1
t
33## f1 t
35** 4i 0 16.87 10i 20 49.7 e
36$$ 5r1 12r2 e
39$$ 1 2 e
51$$ 23r1 22r2 12r3 13r4 16r5 46r6 58r7 27r8 9r9 12r10 t
end
=shell
cp ft03f001 $RTNDIR/xs_delphi.out
end
```

Appendix 4. Matlab script for detector positioning

```
% Geeft coordinaten optimale detectorpositie en afbeelding.
clear all

 X = dlmread('xcoord.txt', '\t', 'A1..A45');
 Y = dlmread('ycoord.txt', '\t', 'A1..A45');
 Z = dlmread('zcoord.txt', '\t', 'A1..A50');

 AWaarden(1,:)= dlmread('fort.2001.txt', '\t', 'A1..A101250');
 BWaarden(1,:)= dlmread('fort.2002.txt', '\t', 'A1..A101250');
 CWaarden(1,:)= dlmread('fort.2003.txt', '\t', 'A1..A101250');
 DWaarden(1,:)= dlmread('fort.2004.txt', '\t', 'A1..A101250');
 EWaarden(1,:)= dlmread('fort.2005.txt', '\t', 'A1..A101250');
 FWaarden(1,:)= dlmread('fort.2006.txt', '\t', 'A1..A101250');
 GWaarden(1,:)= dlmread('fort.2007.txt', '\t', 'A1..A101250');
 HWaarden(1,:)= dlmread('fort.2008.txt', '\t', 'A1..A101250');
 IWaarden(1,:)= dlmread('fort.2009.txt', '\t', 'A1..A101250');
 JWaarden(1,:)= dlmread('fort.2010.txt', '\t', 'A1..A101250');

 Q = zeros(45,45,50);
 R = Q;
 S = Q;
 T = Q;
 U = Q;
 V = Q;
 W = Q;
 L = Q;
 M = Q;
 N = Q;
 TOTAAL = zeros(45,45,50);
 Delen = zeros(45,45,50);
 maxix = 0;
 maxiy = 0;
 maxiz = 0;

 for i = 18:2:28
   for j = 18:2:28
     for k = 1:1:50
       Q(i,j,k) = AWaarden(i+ 45*(j-1)+ 2025*(k-1));
       R(i,j,k) = BWaarden(i+ 45*(j-1)+ 2025*(k-1));
       S(i,j,k) = CWaarden(i+ 45*(j-1)+ 2025*(k-1));
       T(i,j,k) = DWaarden(i+ 45*(j-1)+ 2025*(k-1));
       U(i,j,k) = EWaarden(i+ 45*(j-1)+ 2025*(k-1));
       V(i,j,k) = FWaarden(i+ 45*(j-1)+ 2025*(k-1));
       W(i,j,k) = GWaarden(i+ 45*(j-1)+ 2025*(k-1));
       L(i,j,k) = HWaarden(i+ 45*(j-1)+ 2025*(k-1));
       M(i,j,k) = IWaarden(i+ 45*(j-1)+ 2025*(k-1));
       N(i,j,k) = JWaarden(i+ 45*(j-1)+ 2025*(k-1));
```

```
      TOTAAL(i,j,k) =
abs(Q(i,j,k))+abs(R(i,j,k))+abs(S(i,j,k))+abs(T(i,j,k))+abs(U(i,j,k))+abs(V(i,j,k))+abs(W(i,j,k))+abs(L(i,j,k))+
abs(M(i,j,k))+abs(N(i,j,k));
      Delen(i,j,k) = abs(Q(i,j,k))/TOTAAL(i,j,k);

    end
   end
 end

[num] = max(Delen(:));
[x y z] = ind2sub(size(Delen),find(Delen==num))

 figure(1)
 [x,y,z] = meshgrid(X,Y,Z);
 v = Delen;
 xslice = 52; yslice = 52; zslice = 0;
 slice(x,y,z,v,xslice,yslice,zslice)
 colormap hsv


% figure (2)
%  [x,y,z] = meshgrid(X,Y,Z);
% v = Delen;
% xslice = [0,50,100]; yslice =[49,63]; zslice = [-50,0,50];
% slice(x,y,z,v,xslice,yslice,zslice)
% colormap hsv
```

Bibliography

[1] Berglof, Carl. 'On Measurement and Monitoring of Reactivity in Subcritical Reactor Systems.' Stockholm, 2010.

[2] J. Duderstadt, L. Hamilton. *Nuclear Reactor Analysis*. 1976.

[3] Lathouwers, D. 'Iterative computation of time-eigenvalues of the neutron transport equation.' 2003.

[4] Uhrig, Robert E. *Random Noise Techniques in Nuclear Reactor Systems* . Florida: The Ronald Press Company, 1970.

[5] J.L. Munoz-Cobo, C.Berglof, J. Pena, D. Villamarin, V. Bournos. 'Feynman alpha and Rossi-alpha formulas with spatial and modal effects.' *Annals of Nucelar Energy*, 2010.

[6] Klujber, G. 'Neutron noise measurements on the Delphi subcritical assembly, technical raport.' Budapest, 2011.

[7] Kloosterman, J.L. 'Description of the Delphi subcritical assembly at Delft University of Technology.' Delft, 2003.

[8] W. Uyttenhoven, personal communication, 2011.

[9] Oak Ridge National Laboratory. 'SCALE: A Modular Code System for Performing Standardized Computer Analyses for Licensing Evaluations.' Radiation Safety Information Computational Center at Oak Ridge National Laboratory , January 2009.

[10] B. Boer, D. Lathouwers, M. Ding, J.L. Kloosterman. „Coupled neutronics/ thermal hydraulics calculations for high temperature reactors with the dalton - thermix code system." 2008.

[11] R.B. Lehoucq, D.C. Sorensen, C. Yang. 'Arpack users guide: Solution of large scale eigenvalue problems with implicitly restarted arnoldi methods.' 1997.

[12] N.M. Greene, L.M. Petrie. 'XSDRNPM: A one-dimensional discrete-ordinates code for transport analysis.' OAK RIDGE NATIONAL LABORATORY, september 1998.

[13] G. Klujber, personal communication, 2012.

[14] Wols, Frank. 'Transient analyses of accelerator driven systems using modal expansion techniques.' Delft, 2010.

[15] R.S. Modaka, Anurag Gupta. 'A scheme for the evaluation of dominant time-eigenvalues of a nuclear reactor.' *Annals of Nuclear Energy,* 2007.

[16] The MathWorks, Inc. *Residual Analysis :: Curve Fitting Techniques.* 1984-2007.